



Calhoun: The NPS Institutional Archive
DSpace Repository

Theses and Dissertations

1. Thesis and Dissertation Collection, all items

1983-09

A linear approximation of the source position using multiple MAD

Bock, Wolf-Hubertus

Monterey, California. Naval Postgraduate School

<https://hdl.handle.net/10945/19868>

Downloaded from NPS Archive: Calhoun



Calhoun is the Naval Postgraduate School's public access digital repository for research materials and institutional publications created by the NPS community. Calhoun is named for Professor of Mathematics Guy K. Calhoun, NPS's first appointed -- and published -- scholarly author.

Dudley Knox Library / Naval Postgraduate School
411 Dyer Road / 1 University Circle
Monterey, California USA 93943

<http://www.nps.edu/library>

NAVAL POSTGRADUATE SCHOOL

Monterey, California



THESIS

A LINEAR APPROXIMATION OF THE SOURCE
POSITION USING MULTIPLE MAD

by

Wolf-Hubertus Bock

September 1983

Thesis Advisor: Andrew R. Ochadlick, jr.

Approved for public release; distribution unlimited.

T210144

SECURITY CLASSIFICATION OF THIS PAGE (When Data Entered)

REPORT DOCUMENTATION PAGE		READ INSTRUCTIONS BEFORE COMPLETING FORM
1. REPORT NUMBER	2. GOVT ACCESSION NO.	3. RECIPIENT'S CATALOG NUMBER
4. TITLE (and Subtitle) A Linear Approximation of the Source Position Using Multiple MAD		5. TYPE OF REPORT & PERIOD COVERED Master's Thesis September 1983
7. AUTHOR(s) Wolf-Hubertus Bock		6. PERFORMING ORG. REPORT NUMBER
9. PERFORMING ORGANIZATION NAME AND ADDRESS Naval Postgraduate School Monterey, California 93943		8. CONTRACT OR GRANT NUMBER(s)
11. CONTROLLING OFFICE NAME AND ADDRESS Naval Postgraduate School Monterey, California 93943		10. PROGRAM ELEMENT, PROJECT, TASK AREA & WORK UNIT NUMBERS
14. MONITORING AGENCY NAME & ADDRESS (if different from Controlling Office)		12. REPORT DATE September 1983
		13. NUMBER OF PAGES 61
		15. SECURITY CLASS. (of this report)
		15a. DECLASSIFICATION/DOWNGRADING SCHEDULE
16. DISTRIBUTION STATEMENT (of this Report) Approved for public release; distribution unlimited		
17. DISTRIBUTION STATEMENT (of the abstract entered in Block 20, if different from Report)		
18. SUPPLEMENTARY NOTES		
19. KEY WORDS (Continue on reverse side if necessary and identify by block number) MAD localization, Multiple MAD, Non-acoustic localization		
20. ABSTRACT (Continue on reverse side if necessary and identify by block number) For certain assumptions, an analysis of multiple MAD signals results in a reasonable estimate for the localization of a target relative to the MAD platform. This is achieved by using selective approximations to linearize an initially nonlinear problem. The simulation ignores noise and requires an estimate of the magnitude of the target magnetic moment components. Results indicate that the best localization estimates are		

achieved when the platform is on cardinal headings, and when the target moment has a strong vertical component.

Approved for public release; distribution unlimited.

A Linear Approximation of the Source
Position Using Multiple MAD

by

Wolf-Hubertus Bock
Lieutenant, United States Navy
B.A., Rice University, 1975

Submitted in partial fulfillment of the
requirements for the degree of

MASTER OF SCIENCE IN SYSTEMS TECHNOLOGY
(ANTISUBMARINE WARFARE)

from the

NAVAL POSTGRADUATE SCHOOL
September 1983

no.

Handwritten notes:
B 58315
C 1

ABSTRACT

For certain assumptions, an analysis of multiple MAD signals results in a reasonable estimate for the localization of a target relative to the MAD platform. This is achieved by using selective approximations to linearize an initially nonlinear problem. The simulation ignores noise and requires an estimate of the magnitude of the target magnetic moment components. Results indicate that the best localization estimates are achieved when the platform is on cardinal headings, and when the target moment has a strong vertical component.

TABLE OF CONTENTS

I.	INTRODUCTION	9
	A. BACKGROUND	9
	B. APPROACH	10
II.	THEORY	14
III.	NATURE OF THE PROBLEM	18
IV.	DISCUSSION	23
	A. GENERAL	23
	B. HEADING CHANGES	29
	C. TARGET DIPOLE MOMENT CHANGES	30
	D. CHANGES IN SENSOR SPACING	30
	E. ALTITUDE CHANGES	31
	F. NON-OVERHEAD PASSES	31
	G. AVERAGES	31
	H. IMPORTANCE OF CONSISTENCY	41
	I. IMPLEMENTATION	41
V.	CONCLUSION	42
	APPENDIX A: COMPUTER PROGRAM FOR PLOT OUTPUT	44
	APPENDIX B: COMPUTER PROGRAM FOR NUMERICAL OUTPUT	50
	APPENDIX C: EXAMPLE OUTPUT OF APPENDIX B	55
	APPENDIX D: CRAMER'S RULE	57
	A. GENERAL	57
	B. EXAMPLE	57
	C. SUBROUTINE "CRAMER'S RULE" CHECK	58
	LIST OF REFERENCES	59

BIBLIOGRAPHY 60

INITIAL DISTRIBUTION LIST 61

LIST OF FIGURES

1.1	Spatial Relationship of Sensor Positions	12
1.2	Spatial Relationship of Platform and Target	13
2.1	Vector Relationship of \vec{B}_i , \vec{b}_d , and \vec{B}_e	14
4.1	Initial Run, x position	24
4.2	Initial Run, y position	25
4.3	Initial Run, z position	26
4.4	Initial Run, corrected y position	27
4.5	Platform Heading 60° Magnetic	33
4.6	Platform Heading 120° Magnetic	34
4.7	Platform Heading 240° Magnetic	35
4.8	Platform Heading 300° Magnetic	36
4.9	\vec{m} Vertically Up	37
4.10	\vec{m} Horizontal and Oriented to Magnetic North	38
4.11	\vec{m} Vert. Comp. 50° Down, \vec{m} Hor. Comp. 30° Magnetic	39
4.12	Target at 45° depres. angle rel. to platform at CPA	40

TABLE OF SYMBOLS

\vec{b}_d	magnetic field vector of the target dipole
\vec{B}_e	earth's magnetic field vector
\vec{B}_t	total magnetic field vector
\hat{e}	earth's magnetic field unit vector
e_x, e_y, e_z	components of \hat{e} in cartesian coordinates
\vec{r}	vector from the target to the platform
r	scalar magnitude of \vec{r}

I. INTRODUCTION

A. BACKGROUND

Ever since the operational introduction of the MAD (Magnetic Anomaly Detection) system in 1944, it has been a single sensor system limited to indicating detection only. The short ranges of the early versions allowed a general localization if a signal was detected. The use of multiple sensors should allow for a good estimate of the target's location relative to the sensor platform, assuming that the arrangement of the sensors is such that the received signals are linearly independent of one another. Previous attempts to solve this problem have in general focused on the use of only two sensors, but did not develop a usable solution to operational completion. Work has been done on this topic by Wynn et al., [Ref. 1], using a superconducting gradiometer array. The measured signals in their work were subjected to a novel signal processing technique which, in the laboratory, was used to invert the dipole field equation to determine both the position and the moment vectors of a dipole signal source. This thesis approaches the same problem by simulating five standard total field measurements. As shown in Figure 1.1, four magnetometers moving in parallel paths are used to obtain these measurements. The advantage of this approach compared to that of Wynn et al. is that it utilizes existing technology in conjunction with approximations, delineated in Chapter 3, in order to produce a usable result.

B. APPROACH

The problem of localizing a target from any platform involves at least three unknowns: r_x , r_y , and r_z , the components of the position vector from the platform to the target. In the case of using MAD, three additional unknowns m_x , m_y , and m_z , the components of the target's magnetic moment, are also involved. The result is that there are six unknowns that must be solved for in order to localize a target using MAD. Since a normal sized magnetic target can be approximated by the magnetic field of a dipole [Ref. 2], it was decided to use the dipole equation as described in [Ref. 3] to generate the signals used in this simulation. Equation 1.1 describes the MAD signal, and will be developed from the dipole equation in chapter 2. Equation 1.1 is non-

$$S(\vec{r}) = -(m_x e_x + m_y e_y + m_z e_z) / r^3 + 3(m_x r_x + m_y r_y + m_z r_z)(r_x e_x + r_y e_y + r_z e_z) / r^5 \quad (\text{eqn 1.1})$$

linear in the unknowns. The position vector in equation 1.1 is defined as going from the target to the platform; this is a consequence of using the dipole equation, and will be explained later.

The cartesian coordinates are defined in Figure 1.2. The z axis is in the direction of platform motion, and the y axis is vertical down. The components of the earth's field unit vector, e_x , e_y , and e_z , are assumed to be known quantities. Since it is very difficult to explicitly solve a set of non-linear equations in six unknowns, the problem will be simplified by making assumptions and dividing it into two special cases. The first case is a trivial one in which the target's position is assumed known. For this case, equation 1.1 is linear in the three unknowns m_x , m_y , and m_z . If the three measurements are linearly independent, then Cramer's Rule, [Ref. 4], may be used to solve for these unknowns. The

second case is the more difficult one, and it is the problem investigated in this thesis. In this case, the assumption is made that the target's magnetic moment is known. That reduces equation 1.1 into a non-linear equation in only three unknowns, r_x , r_y , and r_z . If this simplified version of equation 1.1 could be manipulated into a linear form by using several sensors and appropriate combinations of signals, the position of the target could easily be solved for.

This thesis will develop an approximate solution to this problem by using combinations of the total field signals of an idealized multiple MAD system.

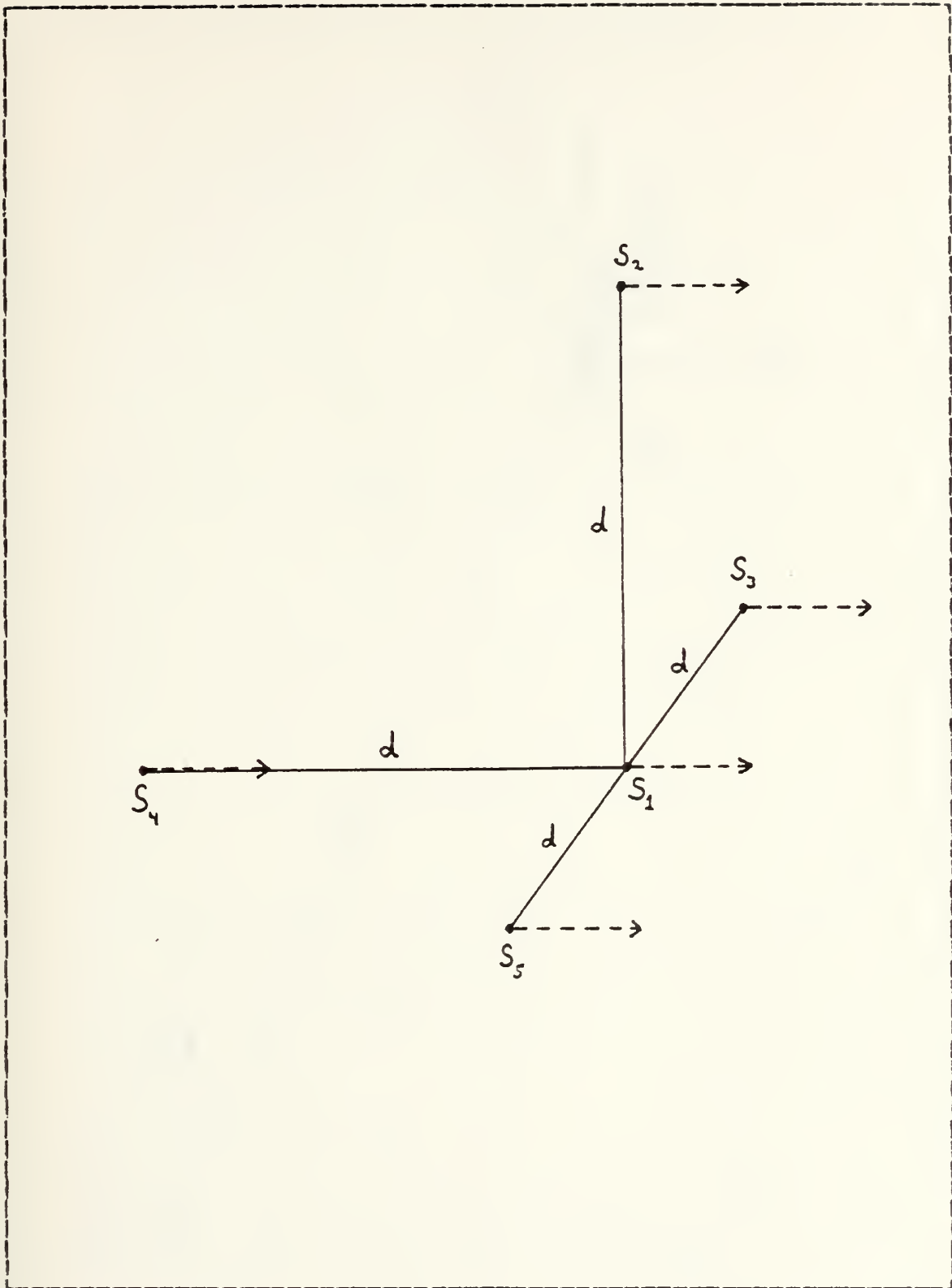


Figure 1.1 Spatial Relationship of Sensor Positions.

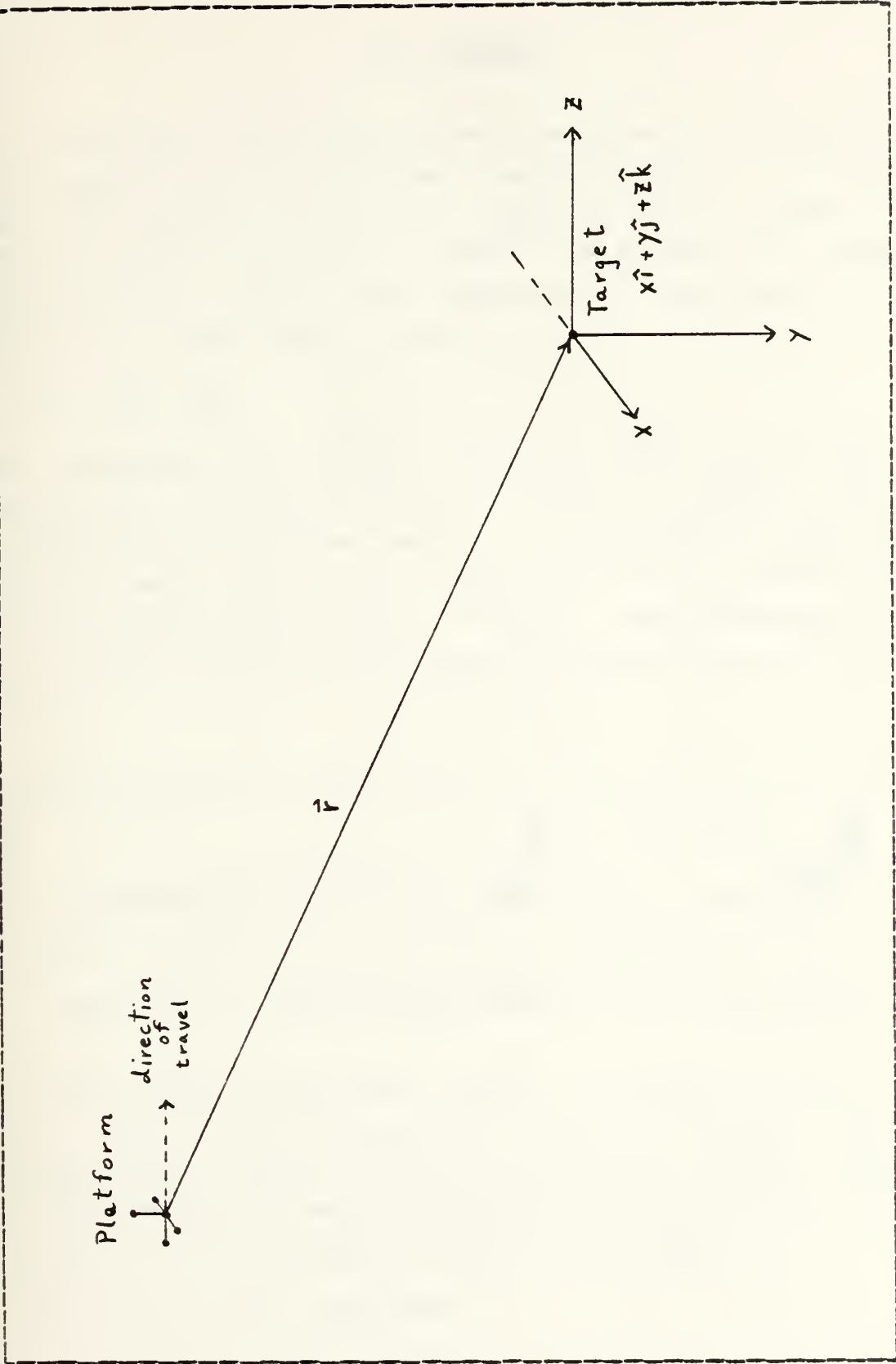


Figure 1.2 Spatial Relationship of Platform and Target.

II. THEORY

The total field magnetometer measures the magnitude of the vector sum of the ambient magnetic field of the earth and the magnetic field of a magnetic dipole moment. The field of the dipole will be used to represent the magnetic field of the target. The magnitude of the vector sum is called the total field as given by

$$\vec{B}_t = |\vec{B}_e + \vec{b}_d|$$

\vec{B}_e represents the earth's magnetic field vector and \vec{b}_d represents the field due to a magnetic dipole. In the general case of interest here, the magnitude of the dipole field is much less than the magnitude of the earth's field. Under certain conditions, a useful approximation to the total field may be derived from the geometry shown in Figure 2.1 .

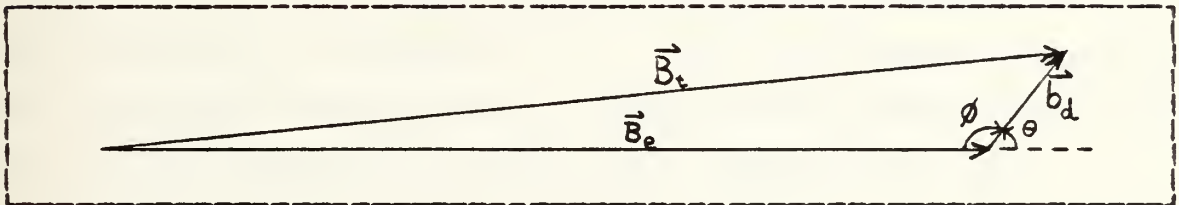


Figure 2.1 Vector Relationship of \vec{B}_t , \vec{b}_d , and \vec{B}_e .

In this figure a very small vector is added to a very large one. The vectors of Figure 2.1 are not to scale. \vec{b}_d is to be considered several orders of magnitude smaller than \vec{B}_e . The application of basic geometric formulas for the sides of a triangle and the angle between sides yields

$$B_t^2 = B_e^2 + b_d^2 - 2b_d B_e \cos\phi$$

for the geometry of Figure 2.1 . In terms of θ this equation becomes

$$B_t^2 = B_e^2 + b_d^2 + 2b_d B_e \cos\theta$$

The B_e^2 term can be factored out of the right hand side of the equation to produce

$$B_t^2 = B_e^2 \{1 + (b_d/B_e)^2 + 2(b_d/B_e) \cos\theta\}$$

Taking the square root yields equation 2.1 .

$$B_t = B_e \{[1 + (b_d/B_e)^2 + 2(b_d/B_e) \cos\theta]^{1/2}\} \quad (\text{eqn 2.1})$$

Since by assumption b_d is much less than B_e , the term $(b_d/B_e)^2$ is much less than $2(b_d/B_e) \cos\theta$ and can be considered negligible. This reduces equation 2.1 to

$$B_t = B_e \{[1 + 2(b_d/B_e) \cos\theta]^{1/2}\} \quad (\text{eqn 2.2})$$

The general expansion formula given by

$$(1+x)^n = 1 + nx + n(n-1)x^2/2! + \text{Higher Order Terms}$$

can be applied to equation 2.1 . For the case here, $n=1/2$, and $x=(b_d/B_e)^2 + 2(b_d/B_e) \cos\theta$. Substituting these values into the general expansion formula gives equation 2.1 as

$$B_t = B_e \{1 + .5[(b_d/B_e)^2 + 2(b_d/B_e) \cos\theta] - 1/8[(b_d/B_e)^2 + (2b_d/B_e) \cos\theta]^2 + \text{H.O.T.}\}$$

Squaring the appropriate term and multiplying through by the coefficients results in

$$B_t = B_e \{1 + .5[(b_d/B_e)^2] + (b_d/B_e) \cos\theta - 1/8[b_d/B_e]^4 - 4/8[b_d/B_e]^3 \cos\theta - 4/8[b_d/B_e]^2 \cos^2\theta + \text{H.O.T.}\}$$

The cubed and higher order terms will be considered to be negligible. Dropping those terms and rearranging the remaining ones yields the form

$$B_t = B_e \{1 + (b_d/B_e) \cos\theta - .5 (b_d/B_e)^2 \cos^2\theta + .5 (b_d/B_e)^2\}$$

Using the relation $\sin^2\theta + \cos^2\theta = 1$, this reduces to

$$B_t = B_e \{1 + (b_d/B_e) \cos\theta + .5 (b_d/B_e)^2 \sin^2\theta\}$$

After multiplying through by B_e , the second term can be written in terms of the dot product $\vec{b}_d \cdot \vec{B}_e / B_e$. This is reduced to $\vec{b}_d \cdot \hat{e}$ if the unit vector \hat{e} is defined as \vec{B}_e / B_e , and the resulting equation is

$$B_t = B_e + \vec{b}_d \cdot \hat{e} + .5 (b_d/B_e)^2 \sin^2\theta$$

Since b_d is on the order of 1nT while B_e is on the order of 50,000 nT, the error term involving the sine is negligible. For the stated assumptions, equation 2.1 can be represented by

$$B_t = B_e + \vec{b}_d \cdot \hat{e} \quad (\text{eqn 2.3})$$

In this thesis, B_e will be assumed constant. In addition, this simulation will assume that no noise exists. Thus, the total field magnetometer will measure the anomaly in the earth's field defined by

$$s(\vec{r}) = \vec{b}_d \cdot \hat{e}$$

In this expression, \vec{b}_d represents the magnetic field of a dipole. \vec{b}_d is defined [Ref. 3] by the equation

$$\vec{b}_d(\vec{r}) = -\vec{m}/r^3 + 3(\vec{m} \cdot \vec{r}) \vec{r}/r^5 \quad (\text{eqn 2.4})$$

\vec{m} is the magnetic dipole moment in units of nTft³. \vec{r} is the position vector to the field point and is measured in feet. If b_d is much less than B_e , then equation 2.3 and equation 2.4 result in the equation

$$S(\vec{r}) = -(\vec{m} \cdot \hat{e})/r^3 + 3(\vec{m} \cdot \vec{r})(\vec{r} \cdot \hat{e})/r^5 \quad (\text{eqn 2.5})$$

This equation is an alternative basis for the derivation of the Anderson's Functions, found in [Ref. 5]. The Anderson Functions are a commonly used approximation for the signal received by a MAD sensor. The computer simulation in this thesis is based on equation 2.5 directly, since it is in a representation which is easier to use than the Anderson's function representation of a MAD signal.

III. NATURE OF THE PROBLEM

This thesis will develop and demonstrate an approximation that generates a reasonable solution of the target's position relative to a platform bearing several "sensors" to "measure" the magnetic signal as the platform makes a straight line encounter near the target. The assumptions are as follows:

- 1.) The dipole equation is a valid representation of the magnetic field of the target.
- 2.) b_d is several orders of magnitude smaller than B_e .
- 3.) Measurements are done using only straight line encounters.
- 4.) The target's magnetic dipole moment is a known vector.
- 5.) The earth magnetic field vector is known.
- 6.) The gradient of the earth's field is zero.
- 7.) No magnetic noise of any kind (environment, sensor, etc) exists.
- 8.) The measurements are oriented along four lines which are oriented with respect to the flight path as shown in Figure 1.1 .

Since the dipole equation is written with the moment at the origin of a coordinate system, the calculations of the signal field values used in the simulation are made with the target located at the origin. As will be seen, the program performs a coordinate transformation in order to produce the output of target position relative to the platform. After this coordinate transformation, the origin is located at the sensor platform and moves with it.

The five measurements are made along four separate flight paths, so only four different "sensors" are involved.

Sensor 4 could be replaced by inducing a time delay in the measurement of sensor 1. The signals generated at these measurement points are measured at each time step. The position vectors can all be described relative to the origin, located at the target, in terms of the position vector of sensor 1. The measured signals are represented by the following equations:

$$\begin{aligned}
 S(\vec{r}_1) &= - \{ (m_x e_x + m_y e_y + m_z e_z) (r_1)^2 - 3 (m_x + m_y + m_z) (x e_x + y e_y + z e_z) \} / r_1^5 \\
 S(\vec{r}_2) &= - \{ (m_x e_x + m_y e_y + m_z e_z) (r_2)^2 - 3 (m_x + m_y [y-d] + m_z) (x e_x + [y-d] e_y + z e_z) \} / r_2^5 \\
 S(\vec{r}_3) &= - \{ (m_x e_x + m_y e_y + m_z e_z) (r_3)^2 - 3 (m_x [x-d] + m_y + m_z) ([x-d] e_x + y e_y + z e_z) \} / r_3^5 \\
 S(\vec{r}_4) &= - \{ (m_x e_x + m_y e_y + m_z e_z) (r_4)^2 - 3 (m_x + m_y + m_z [z-d]) (x e_x + y e_y + [z-d] e_z) \} / r_4^5 \\
 S(\vec{r}_5) &= - \{ (m_x e_x + m_y e_y + m_z e_z) (r_5)^2 - 3 (m_x [x+d] + m_y + m_z) ([x+d] e_x + y e_y + z e_z) \} / r_5^5
 \end{aligned}$$

For convenience, the following dummy variables are used in the computer program and are defined as:

$$\begin{aligned}
 G &= m_x e_x + m_y e_y + m_z e_z \\
 V1 &= 3m_x e_x - G \\
 V2 &= 3(m_x e_y + m_y e_x) \\
 V3 &= 3m_y e_y - G \\
 V4 &= 3(m_y e_z + m_z e_y) \\
 V5 &= 3m_z e_z - G \\
 V6 &= 3(m_z e_x - m_x e_z) \\
 S1 &= S(\vec{r}_1) \\
 S2 &= S(\vec{r}_2) \\
 S3 &= S(\vec{r}_3) \\
 S4 &= S(\vec{r}_4) \\
 S5 &= S(\vec{r}_5)
 \end{aligned}$$

The use of these variables reduces the above equations to the following form, which are the defining equations for the signals in the simulation.

$$S1 = (V1x^2 + V2xy + V3y^2 + V4yz + V5z^2 + V6xz) / r^5$$

$$S_2 = (V_1x^2 + V_2xy - V_2xd + V_3y^2 - 2V_3yd + V_3d^2 + V_4yz - V_4dz + V_5z^2 + V_6xz) / r_2^5$$

$$S_3 = (V_1x^2 - 2V_1xd + V_1d^2 + V_2xy - V_2dy + V_3y^2 + V_4yz + V_5z^2 + V_6xz - V_6dz) / r_3^5$$

$$S_4 = (V_1x^2 + V_2xy + V_3y^2 + V_4yz - V_4yd + V_5z^2 - 2V_5zd + V_5d^2 + V_6xz - V_6xd) / r_4^5$$

$$S_5 = (V_1x^2 + 2V_1xd + V_1d^2 + V_2xy + V_2dy + V_3y^2 + V_4yz + V_5z^2 + V_6xz + V_6dz) / r_5^5$$

The unknowns of interest are x , y , and z , which are related to the position vectors as follows:

$$\vec{r}_1 = x\hat{i} + y\hat{j} + z\hat{k} \quad (\text{eqn 3.1})$$

$$\vec{r}_2 = x\hat{i} + (y-d)\hat{j} + z\hat{k} \quad (\text{eqn 3.2})$$

$$\vec{r}_3 = (x-d)\hat{i} + y\hat{j} + z\hat{k} \quad (\text{eqn 3.3})$$

$$\vec{r}_4 = x\hat{i} + y\hat{j} + (z-d)\hat{k} \quad (\text{eqn 3.4})$$

$$\vec{r}_5 = (x+d)\hat{i} + y\hat{j} + z\hat{k} \quad (\text{eqn 3.5})$$

To linearize the problem it will be assumed that the denominators of the equations for S_1 , S_2 , S_3 , S_4 , and S_5 given above are all equal to r , i.e.,

$$r = r_1 = r_2 = r_3 = r_4 = r_5$$

The equations for S_1 , S_2 , S_3 , S_4 , and S_5 with the denominators equal can then be subtracted from one another to yield the following:

$$S_2 - S_3 = \{(V_2 - 2V_1)x + (2V_3 - V_2)y + (V_4 - V_6)z + (V_1 - V_3)d\} (-d/r^5)$$

$$S_2 - S_5 = \{(V_2 + 2V_1)x + (2V_3 + V_2)y + (V_4 + V_6)z + (V_1 - V_3)d\} (-d/r^5)$$

$$S_3 - S_1 = \{2V_1x + V_2y + V_6z - V_1d\} (-d/r^5)$$

$$S_5 - S_1 = \{-2V_1x - V_2y - V_6z - V_1d\} (-d/r^5)$$

$$S_3 - S_4 = \{(2V_1 - V_6)x + (V_2 - V_4)y + (V_6 - 2V_5)z + (V_5 - V_1)d\} (-d/r^5)$$

$$S_5 - S_4 = \{-(2V_1 + V_6)x - (V_2 + V_4)y - (V_6 + 2V_5)z + (V_5 - V_1)d\} (-d/r^5)$$

Since the denominators are assumed to be identical, if these six equations are divided in pairs the coefficients involving the non-linear r^5 term and the quantity d are canceled out. This results in the following equations that define the new variables A_1 , A_2 , and A_3 as

$$A_1 = (S_2 - S_3) / (S_2 - S_5) \quad (\text{eqn 3.6})$$

$$A_2 = (S_3 - S_1) / (S_5 - S_1) \quad (\text{eqn 3.7})$$

$$A_3 = (S_3 - S_4) / (S_5 - S_4) \quad (\text{eqn 3.8})$$

Defining the following variables for convenience,

$$C1 = A1(V2+2V1) - (V2-2V1)$$

$$C2 = A1(2V3+V2) - (2V3-V2)$$

$$C3 = A1(V4+V6) - (V4-V6)$$

$$K1 = [(V1-V3) - A1(V1-V3)]d$$

$$C4 = A2(2V1) + 2V1$$

$$C5 = A2(V2) + V2$$

$$C6 = A2(V6) + V6$$

$$K2 = [V1 - A2(V1)]d$$

$$C7 = A3(V6+2V1) - (V6-2V1)$$

$$C8 = A3(V4+V2) - (V4-V2)$$

$$C9 = A3(2V5+V6) - (2V5-V6)$$

$$K3 = [(V1-V5) - A3(V1-V5)]d$$

equations 3.6 - 3.8 can be written in the following form as

$$C1x + C2y + C3z = K1 \quad (\text{eqn 3.9})$$

$$C4x + C5y + C6z = K2 \quad (\text{eqn 3.10})$$

$$C7x + C8y + C9z = K3 \quad (\text{eqn 3.11})$$

These three equations are linear in terms of x , y , and z . In addition, they are linearly independent as shown by using the program in Appendix B. A sample output demonstrating the linear independence is shown in Appendix C. Since they are linearly independent, Cramer's Rule can be used to solve equations 3.9 - 3.11 for x , y , and z . The computer program in Appendix A was written in terms of these equations. The program assumes that the magnitude of the target's magnetic moment is 5×10^8 nTft³. A representative moment was selected by using the values listed by Fromm in [Ref. 2], who lists a moment of 10^8 to 2×10^8 cgs units for a submarine. One cgs unit is approximately 3.35 nTft³. The value used in the program is a rounded out average of Fromm's values. Computations are done using the standard convention with the target dipole at the origin. However, as indicated earlier,

the output is corrected by a coordinate transformation so that the platform is at the origin, and the target position is given with respect to the platform.

IV. DISCUSSION

A. GENERAL

The program in Appendix B was written to check whether the results generated by the approximation equations were reasonably close to the actual coordinates of the target. The program was modified into the form shown in Appendix A to graphically provide a comparison between the calculated and the actual position coordinates. Initial parameters for the knowns in the equations were a platform heading of 30° magnetic, an earth field vector of 70° down from the horizontal, and a target dipole moment vector with a vertical component 50° down from the horizontal and a horizontal component oriented 355° from magnetic north. These initial parameters have no special significance, and merely represent a convenient starting point. As discussed earlier, the magnitude of the target dipole moment was set at the value of 5×10^8 nTft³. The spacing between measurement positions, d , was taken as 50 feet, and the platform passed directly overhead the target at 1000 feet. This and all subsequent runs were started at 5000 feet prior to CPA (closest point of approach) with the platform advancing 50 feet per time step. One position calculation was completed at each time step, the simulation ceasing when the platform was 5000 feet past CPA. For interpretation purposes, calculated target positions are shown as the sensor platform moves 10,000 feet past the target in a straight line encounter, with CPA occurring at the 5000 foot point. Neither the CPA nor the target's location are in any way considered known in the localization process. However, as the area of interest is the behavior of the simulation close to CPA, the closest

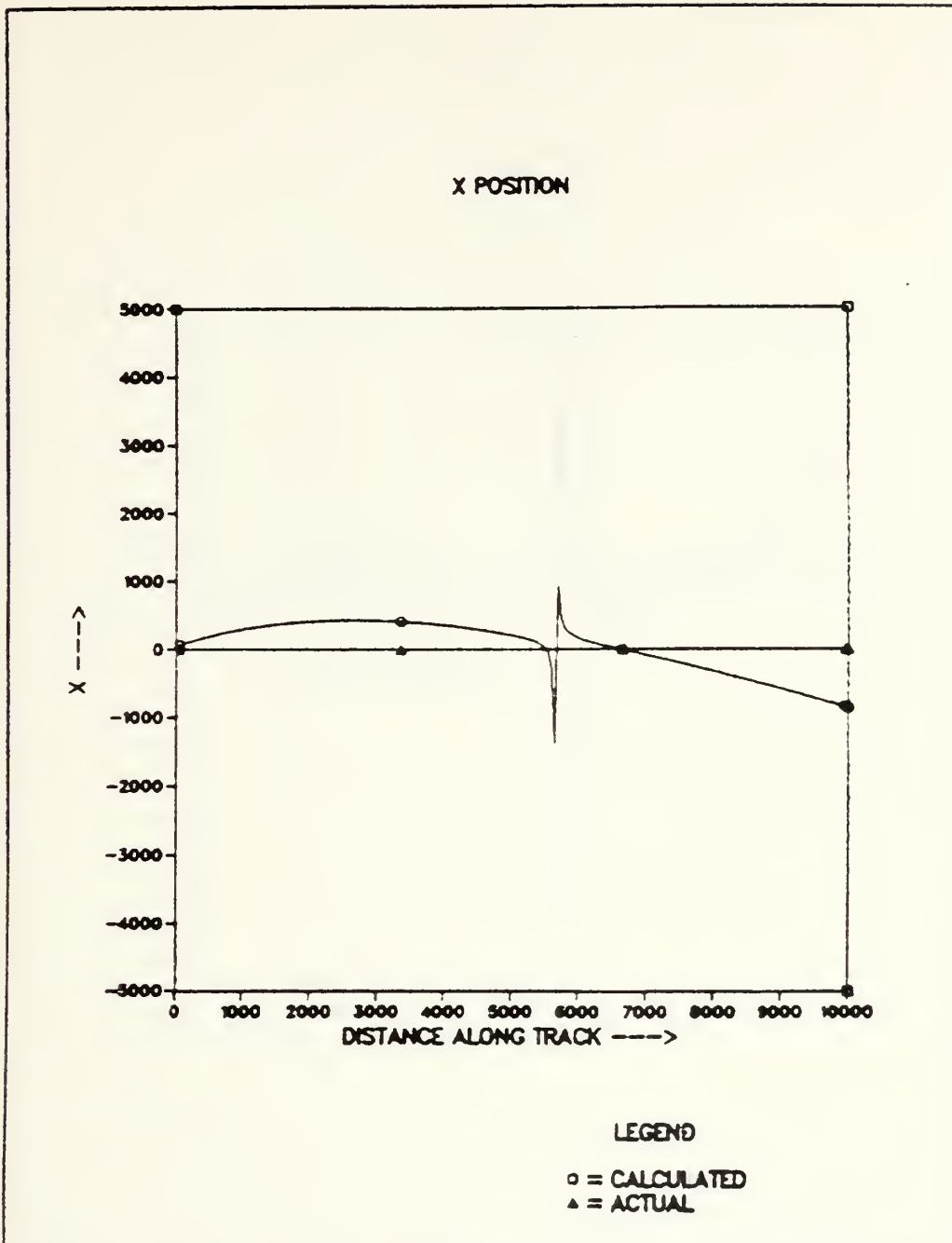


Figure 4.1 Initial Run, x position.

point of approach is always centered in the following figures.

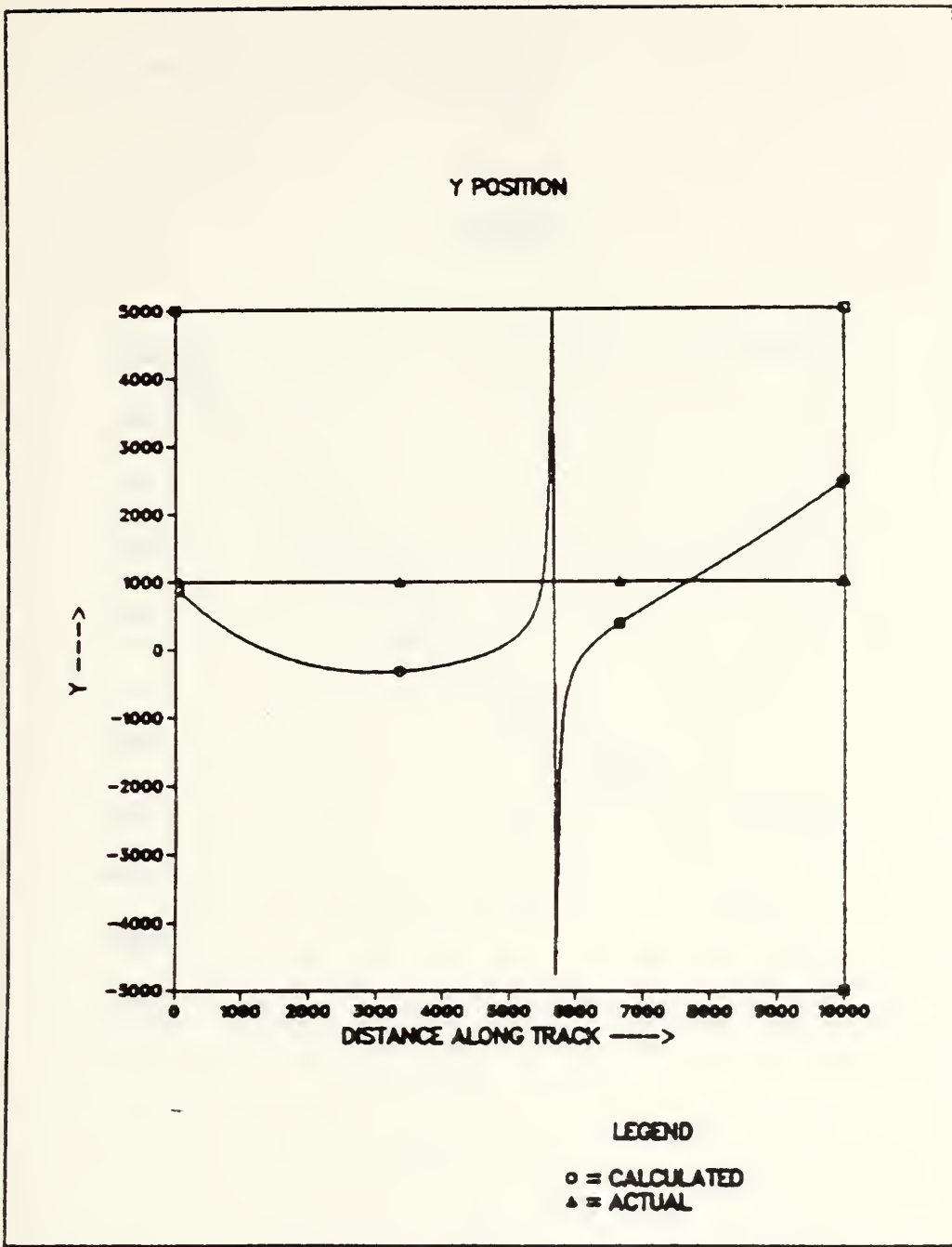


Figure 4.2 Initial Run, y position.

From the orientation of the coordinate system shown in Figure 1.2, z is in the direction of flight, y is straight down, and x is off the right side of the platform. Since

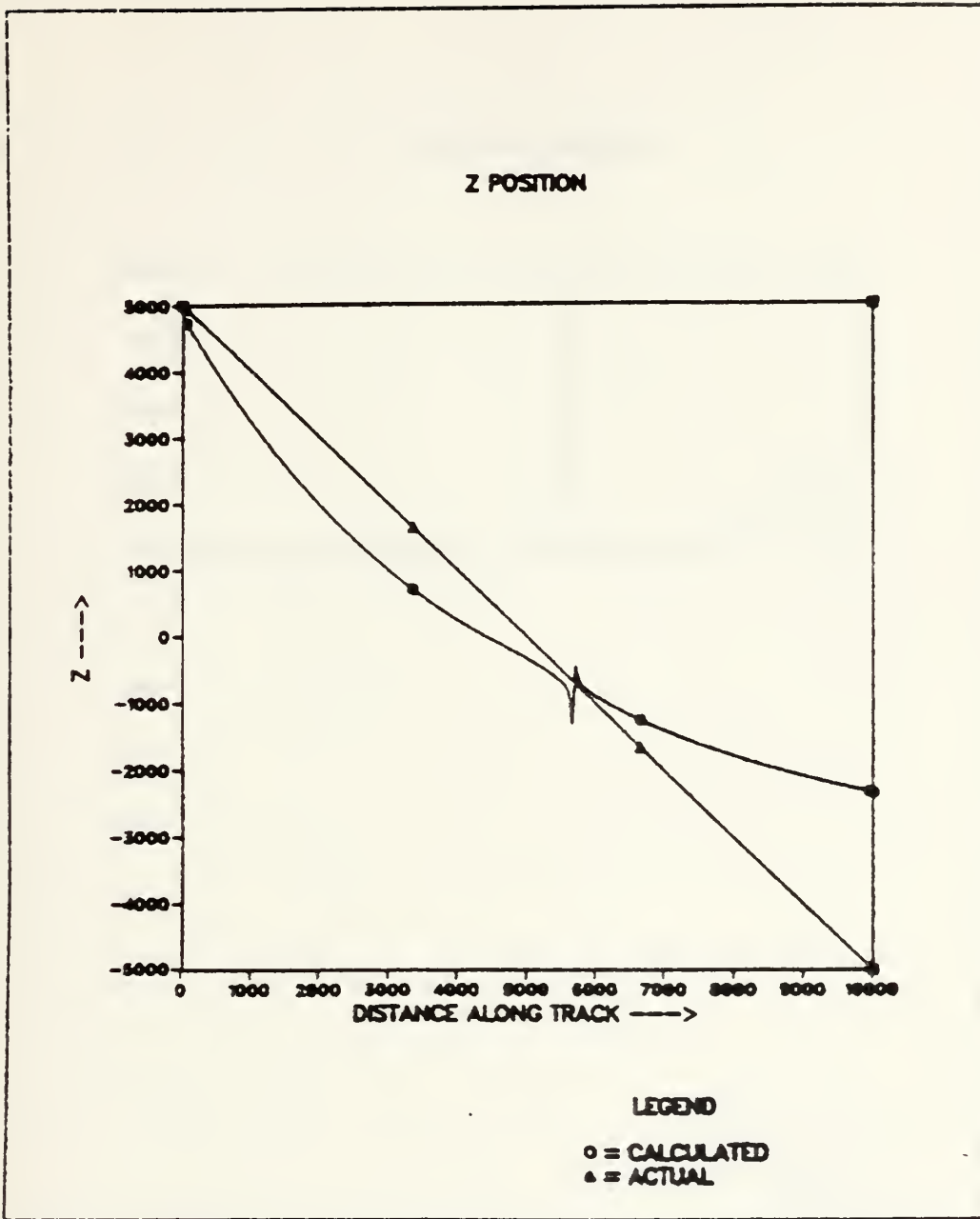


Figure 4.3 Initial Run, z position.

this thesis investigates straight line encounters only, the $x(\text{actual})$ and $y(\text{actual})$ coordinates will remain constant throughout any run for the coordinate orientation used. The

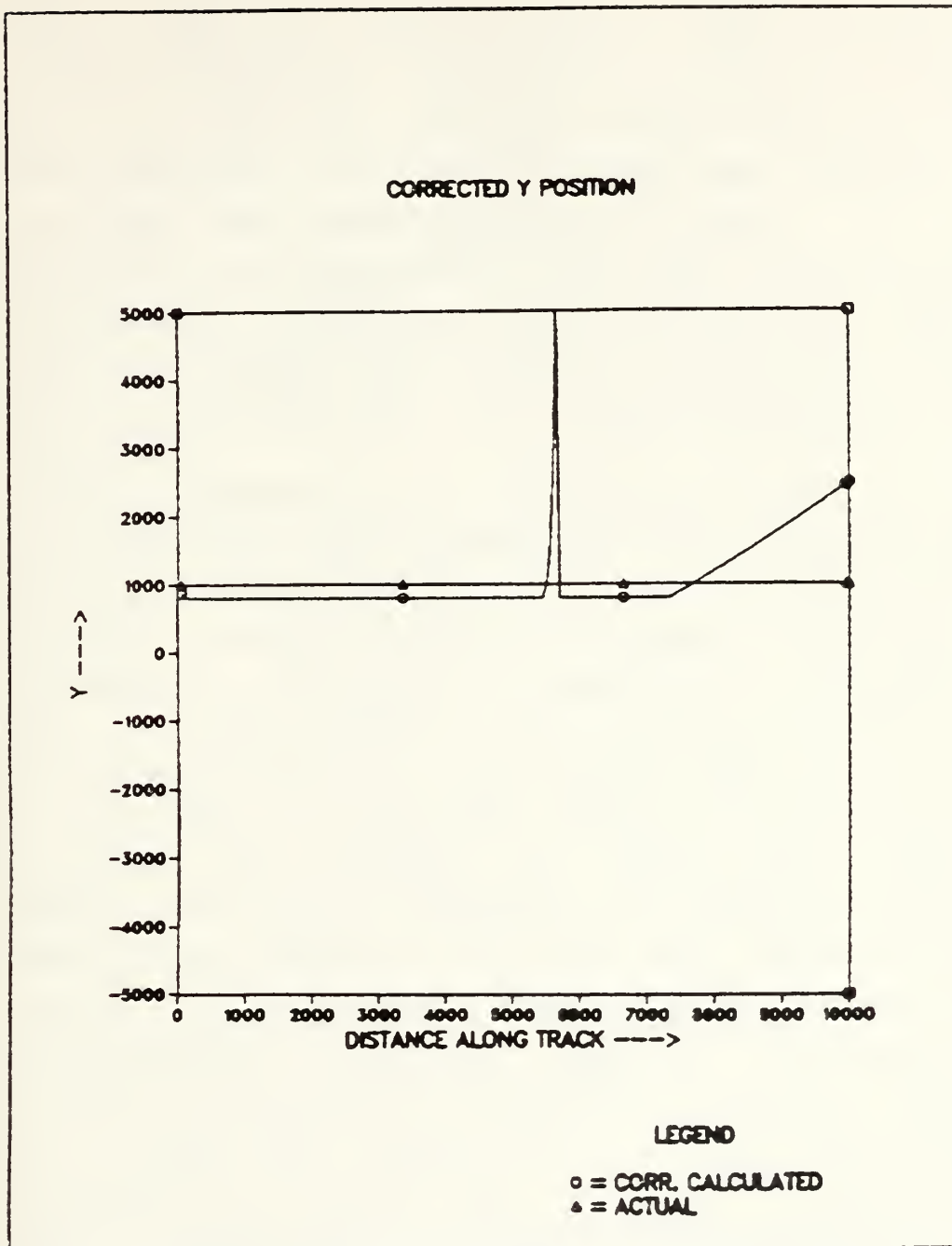


Figure 4.4 Initial Run, corrected y position.

five measurements will therefore be made with their respective x and y coordinates as constants. The z coordinate will vary. This means that for the initial pass described,

x(actual) would be constant at zero, y(actual) would be constant at 1000 feet, while z(actual) would progress from 5000 feet to -5000 feet. Figures 4.1 - 4.3 show a comparison of the actual and calculated target positions as the platform completes the initial run described earlier. It will be noted that the calculated and actual x, y, and z positions are almost identical at the start of the run. This is a coincidence. "Crossover" points such as this occur for all three coordinates simultaneously during a run, falling closer or further away from CPA, depending upon the choice of parameters.

In this initial run, it is obvious that the "worst" estimates occur for the y coordinate. This is less significant than it seems at first glance, however, as the y coordinate is the vertical separation between the platform and the target. If the target is submerged, this value is unknown, but the altitude of the platform is known. The target can be no closer to the platform than this altitude, since the target is physically unable to rise above the ocean surface. As an example, if a target depth of 200 feet is assumed, the initial y separation of 1000 feet forces the altitude in this simulation to be 800 feet. Using this value as a bound on y, it can be seen in Figure 4.4 that the y calculated position is somewhat improved. Accordingly, it seems that the particular arrangements of sensors shown in Figure 1.1 does show promise in the problem of utilizing this geometry of Multiple MAD for accurate localization purposes. Accordingly, variations of parameters were tried in order to determine what effect changing them would have. In all cases, parameters not specifically mentioned in a section will retain the values as for the initial run described above. The singularity-like behavior occurring at various places on the graphs are a result of the determinant of the denominator in the Cramer's Rule subroutine having a value close to zero.

B. HEADING CHANGES

In this section, the localization process will be investigated as a function of heading. Compared to the initial conditions described above, the crossover points were found to be moved further out past 5000 feet prior to CPA on a heading of 0° . While a specific example of this is not shown, the behavior of the crossover points for the platform headings of 30° and 60° may be observed by comparing Figures 4.1 - 4.4 to the respective portions of Figure 4.5. The x position estimates were better for a North-South heading than for any other platform heading, although the estimates on East-West headings were also very good. For a 90° heading there are two crossover points located equidistant at 1200 feet from CPA. Calculated positions on all headings are generally good, excepting those around 60° , where the x estimates shows a large discrepancy at distances greater than 3000 feet prior to CPA. The y estimates are not significantly affected, but the z estimates are good only within ± 1200 feet of CPA. Nevertheless, even in this worst-case situation, reasonable calculated coordinates are available for localization along a significant portion of the track.

As shown in Figures 4.5 - 4.8, headings in the quadrant $0^\circ - 90^\circ$ reasonably describe what happens on any heading, as the graphs for analogous headings (50° , 120° , 240° , and 300° in this example) have similar shapes, although the orientation may differ between quadrants. These similarities are apparently due to the fact that analogous heading in quadrants 1 and 3 and quadrants 2 and 4 are in fact reciprocal headings, and so one would expect the graphs to maintain the same shape; however, the ending point of one would represent the starting point of the other. The relationship between adjacent quadrants probably exists for similar reasons.

C. TARGET DIPOLE MOMENT CHANGES

In this section, the horizontal component of \vec{m} was oriented in the 0° (magnetic North) direction vice 355° , and the vertical component of \vec{m} was varied. The best positioning was obtained for \vec{m} oriented vertically up, i.e., no horizontal component, and an example for that case is shown in figure 4.9. Poor positioning was obtained for the vertical component of \vec{m} pointing between the horizontal and 45° up. The worst case shown is Figure 4.10, where \vec{m} is oriented horizontally pointing due north. With the moment oriented at an angle below the horizontal, reasonable positioning estimates were obtained. There was less variability in positioning for moments pointing below the horizontal than for those pointing above the horizontal.

The results for variations in the orientation of the target dipole moment suggests that the positioning estimates are less sensitive to moment orientation changes in the horizontal plane as compared to the vertical plane. For example, by keeping the vertical component of \vec{m} constant at an angle of 50° down while varying the horizontal component direction it was found that the horizontal component affected the positioning much less than variations in the vertical. Illustrated in Figure 4.11, the x estimates of position improve as the horizontal component approaches the platform heading, while the y estimates improve as the horizontal component approaches alignment with magnetic North. The latter case is not shown.

D. CHANGES IN SENSOR SPACING

Changing the inter-sensor spacing had at most a weak effect upon the position output, even with spacing as short as 5 feet or as long as 200 feet. This would be expected in a computer simulation where sufficient precision is

available. For a spacing as great as 1000 feet some effect became noticeable. In the real world, sensor spacing would influence the localization estimates.

E. ALTITUDE CHANGES

For a straight overhead pass, positioning information appears best if a pass with a 500 to 1000 foot separation between the target and the platform is made at CPA. At greater altitudes, the accuracy suffers slightly with the increase in altitude, while at lesser ranges, usable positioning information is obtained only relatively close to CPA. For example, for a vertical separation of 400 feet, positioning data was very inaccurate at slant ranges greater than 1000 feet.

F. NON-OVERHEAD PASSES

This program gives poor results for passes that are not directly over or directly off to one side of the target. The worst situation observed in any variation is illustrated in Figure 4.12. To generate this figure, a pass was made such that the actual x coordinate was approximately equal to the actual y coordinate. The best positioning was achieved by overhead passes, but low off to the side passes can yield good results as well.

G. AVERAGES

The averages resulting from a number of runs are presented in Table I. These selected averages, covering all of the variations discussed in this chapter, show little consistency. This is probably due in part to the existence of the singularities. The variability is also a function of the limits of travel for the runs. Nevertheless, for most

TABLE I

Values of x and y Averaged over a Run

Run	hdq	d	$\frac{avq}{x}$	$\frac{avq}{y}$	$\frac{avq}{x}$	$\frac{avq}{y}$	$\frac{avq}{x}$	$\frac{avq}{y}$
1	300	50	500	-50	0	42	1000	480
2	00	500	500	-500	0	-17	1000	651
3	150	500	500	-500	0	19	1000	548
4	450	500	500	-500	0	-296	1000	893
5	600	500	500	-500	0	302	1000	-248
6	750	500	500	-500	0	244	1000	-185
7	900	500	500	-500	0	222	1000	-169
8	1200	500	500	-500	0	326	1000	-217
9	1500	500	500	-500	0	96	1000	385
10	1800	500	500	-500	0	11	1000	539
11	2250	500	500	-500	0	244	1000	825
12	2700	500	500	-500	0	-219	1000	-167
13	3150	500	500	-500	0	-10	1000	585
14	3300	500	500	-500	0	26	1000	494
15	3300	500	700	000	0	-96	1000	1025
16	900	500	700	000	0	384	1000	-532
17	3300	500	-900	000	0	-199	1000	-796
18	3300	500	-450	000	0	-206	1000	-674
19	3300	500	000	000	0	-8	1000	-13
20	3300	500	900	000	0	199	1000	-797
21	3300	500	500	000	0	79	1000	462
22	3300	500	500	000	0	102	1000	631
23	3300	500	500	000	0	66	1000	993
24	3300	500	500	-940	0	383	1000	-270
25	3300	500	500	-940	0	376	1000	-321
26	3300	500	500	-500	436	412	900	1690
27	3300	500	500	-500	500	-180	300	199
28	3300	500	500	-500	714	-116	700	848
29	3300	500	500	-500	800	-255	600	911
30	3300	500	500	-500	857	-501	500	-440
31	3300	500	500	-500	917	-412	400	-423
32	3300	500	500	-500	954	-147	300	-2025
33	3300	500	500	-500	980	944	200	-186
34	3300	500	500	-500	994	797	100	-1665
35	3300	500	500	-500	1000	813	0	-1471
36	3300	500	500	-500	500	-478	600	538
37	3300	500	500	-500	500	-345	800	492
38	3300	500	500	-500	0	37	1000	466
39	3300	500	500	-500	0	37	1000	461
40	3300	500	500	-500	0	38	1000	470
41	3300	500	500	-500	0	45	1000	490
42	3300	500	500	-500	0	48	1000	500
43	3300	100	500	-500	0	-193	1000	759
44	3300	500	500	-500	0	-66	800	662
45	3300	500	500	-500	0	-238	600	1058
46	3300	500	500	-500	0	870	400	1757
47	3300	500	500	-500	0	390	200	263
48	3300	500	500	-500	0	108	1200	372
49	3300	500	500	-500	0	219	1400	246
50	3300	500	500	-500	0	266	1600	192
51	3300	500	500	-500	0	313	1800	152
52	3300	500	500	-500	0	410	2000	72
53	3300	500	-450	000	0	275	1000	-344
54	3300	500	000	000	0	138	1000	140
55	3300	500	-450	000	0	-226	1000	-693
56	3300	500	-450	000	0	584	1000	-785
57	3300	500	000	000	0	802	1000	19
58	3300	500	450	-450	0	332	1000	-201

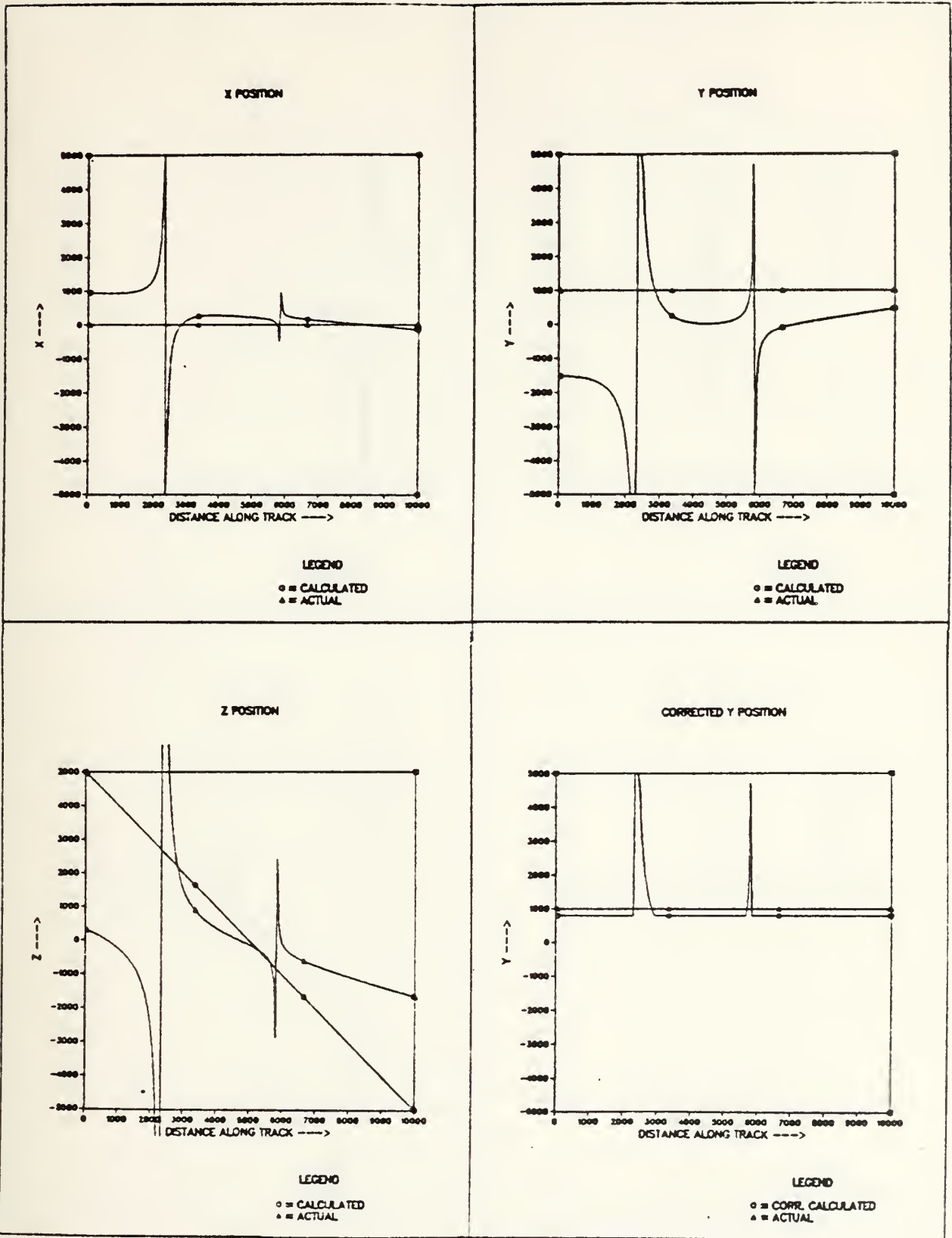


Figure 4.5 Platform Heading 60° Magnetic.

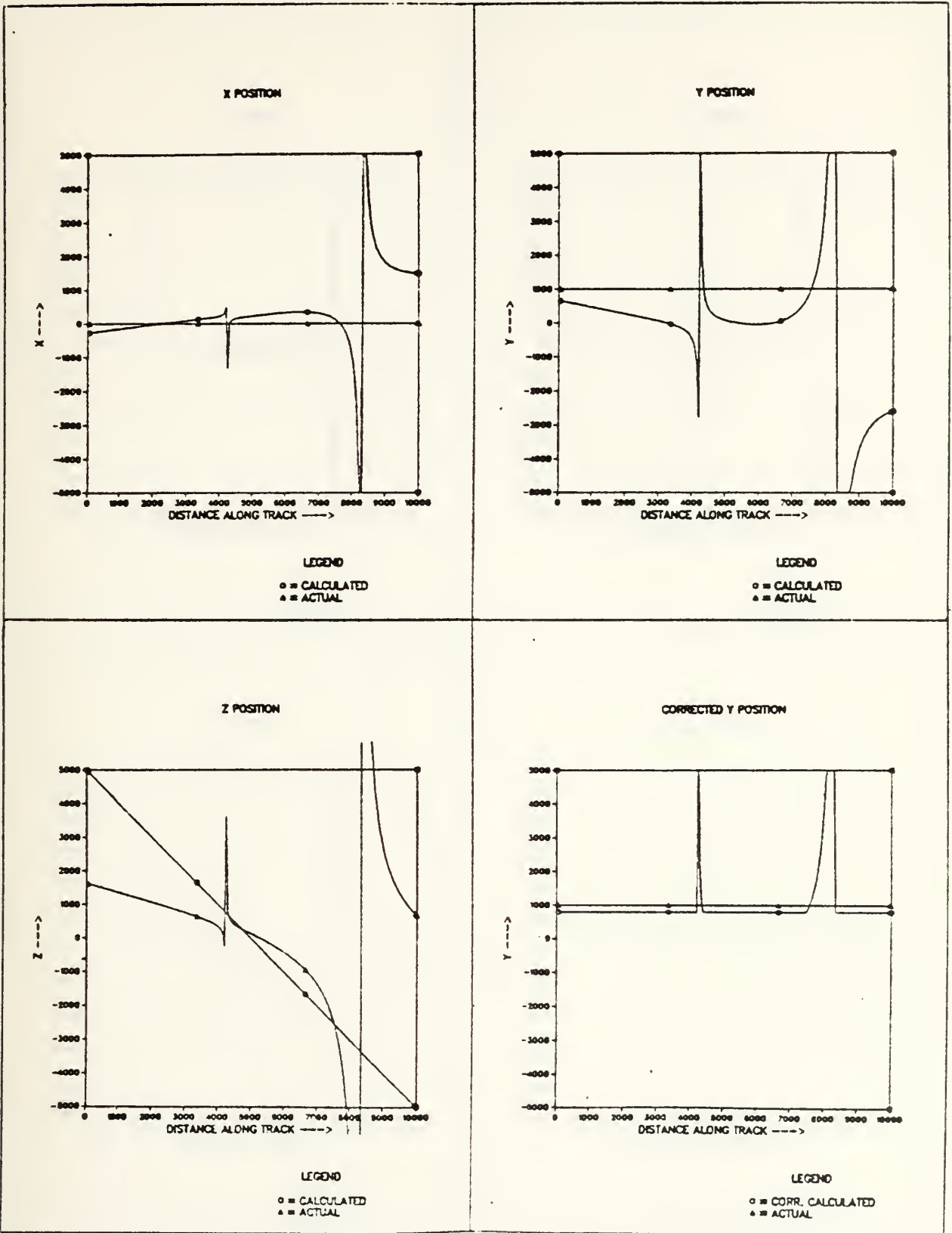


Figure 4.6 Platform Heading 120° Magnetic.

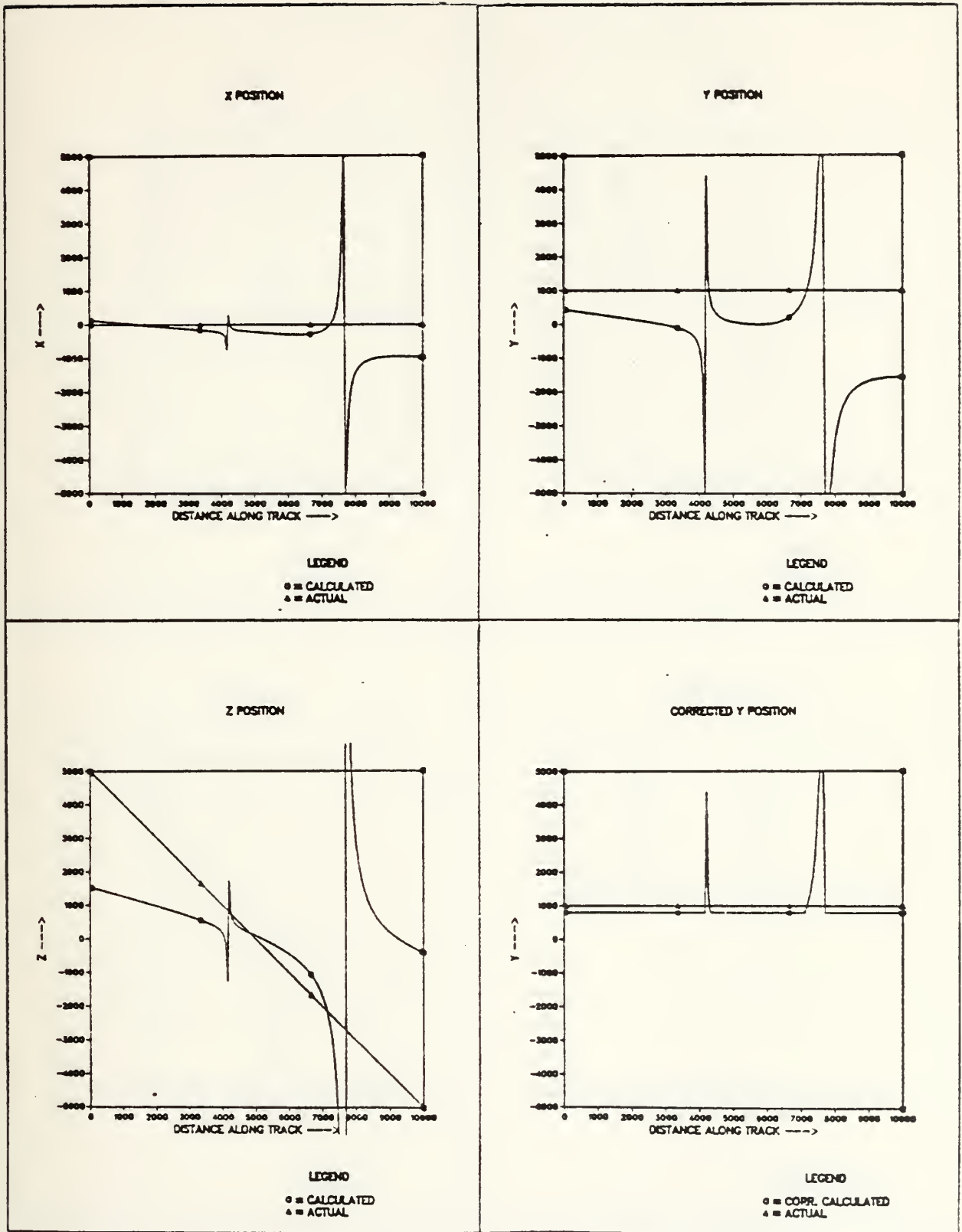


Figure 4.7 Platform Heading 240° Magnetic.

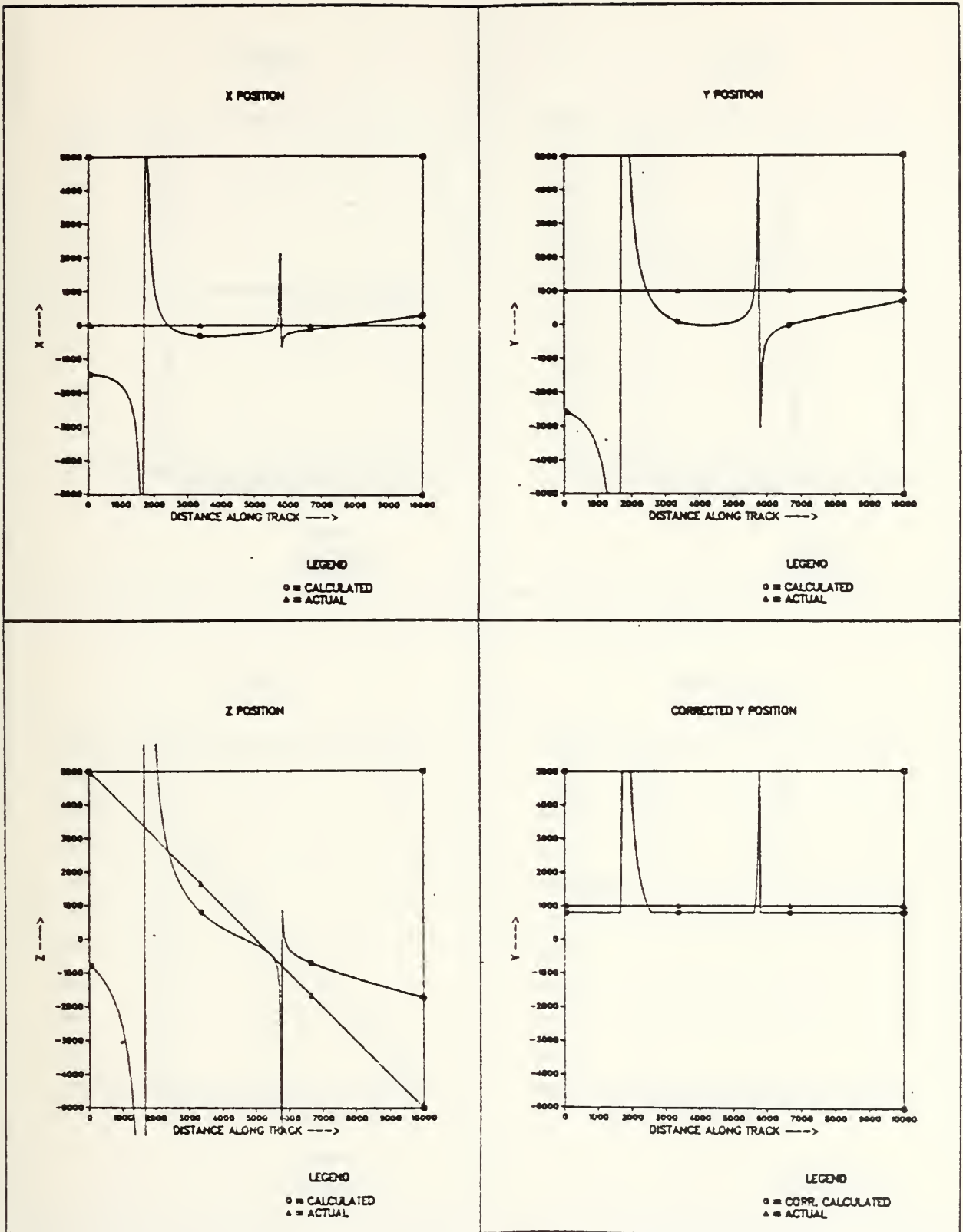


Figure 4.8 Platform Heading 300° Magnetic.

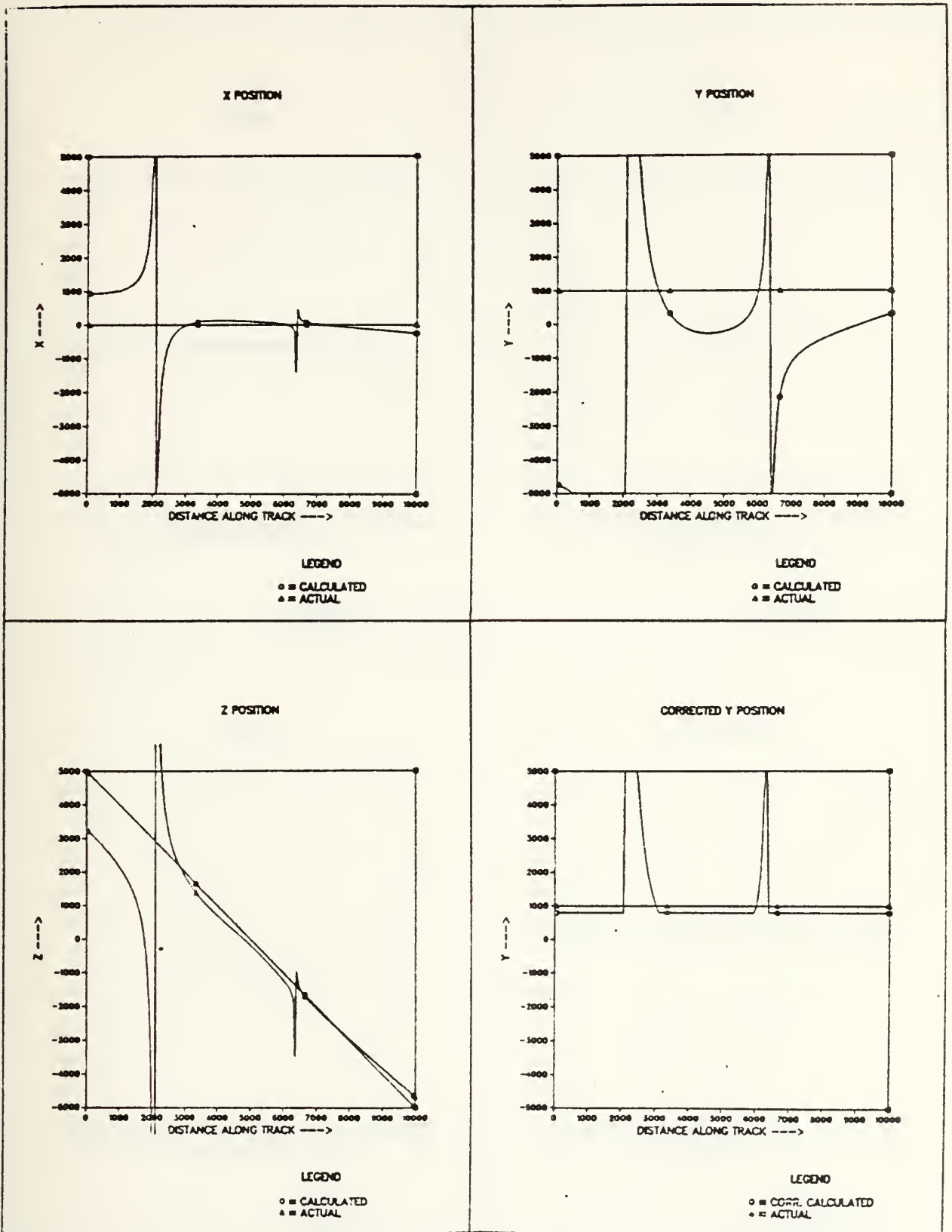


Figure 4.9 \vec{m} Vertically Up.

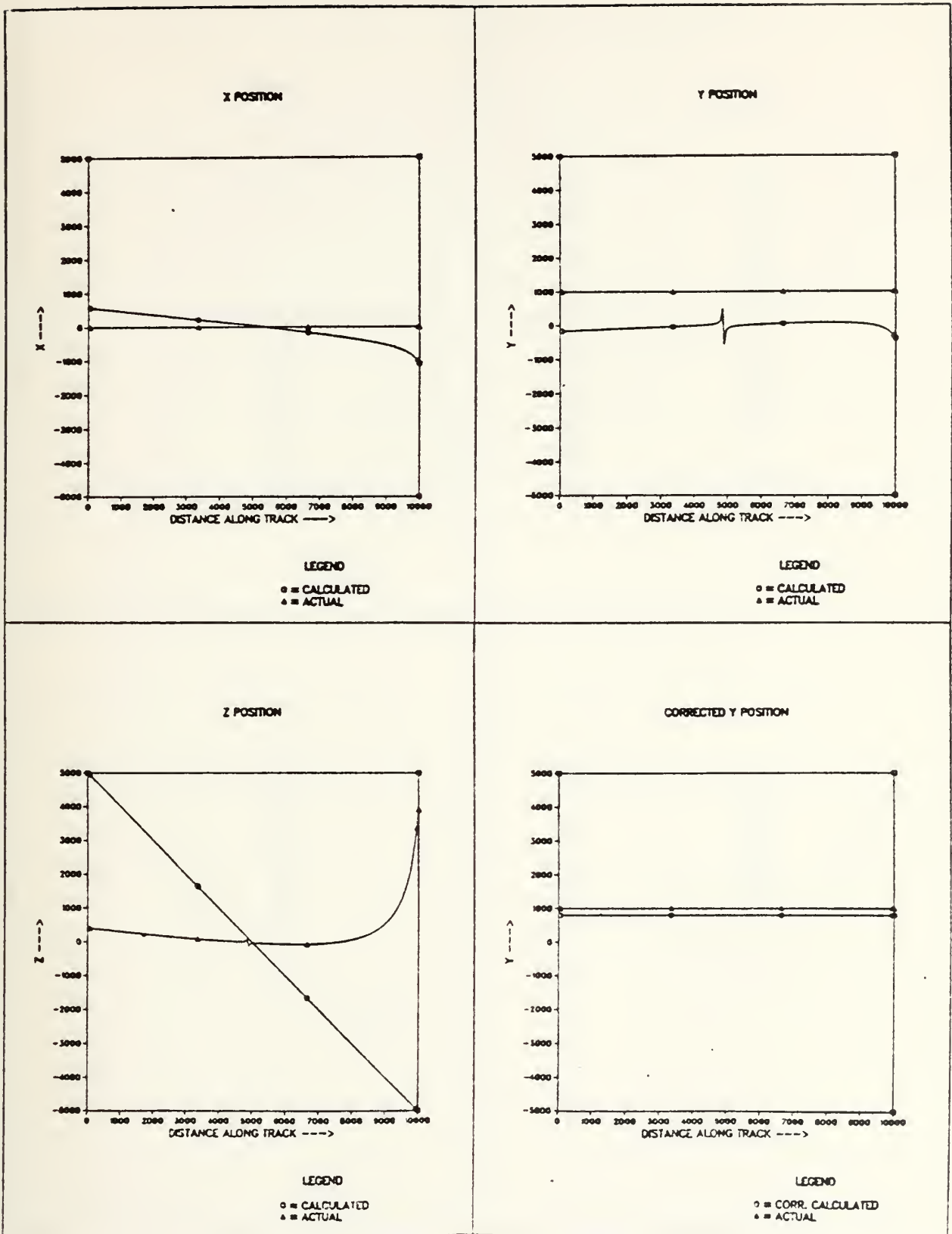


Figure 4.10 \vec{m} Horizontal and Oriented to Magnetic North.

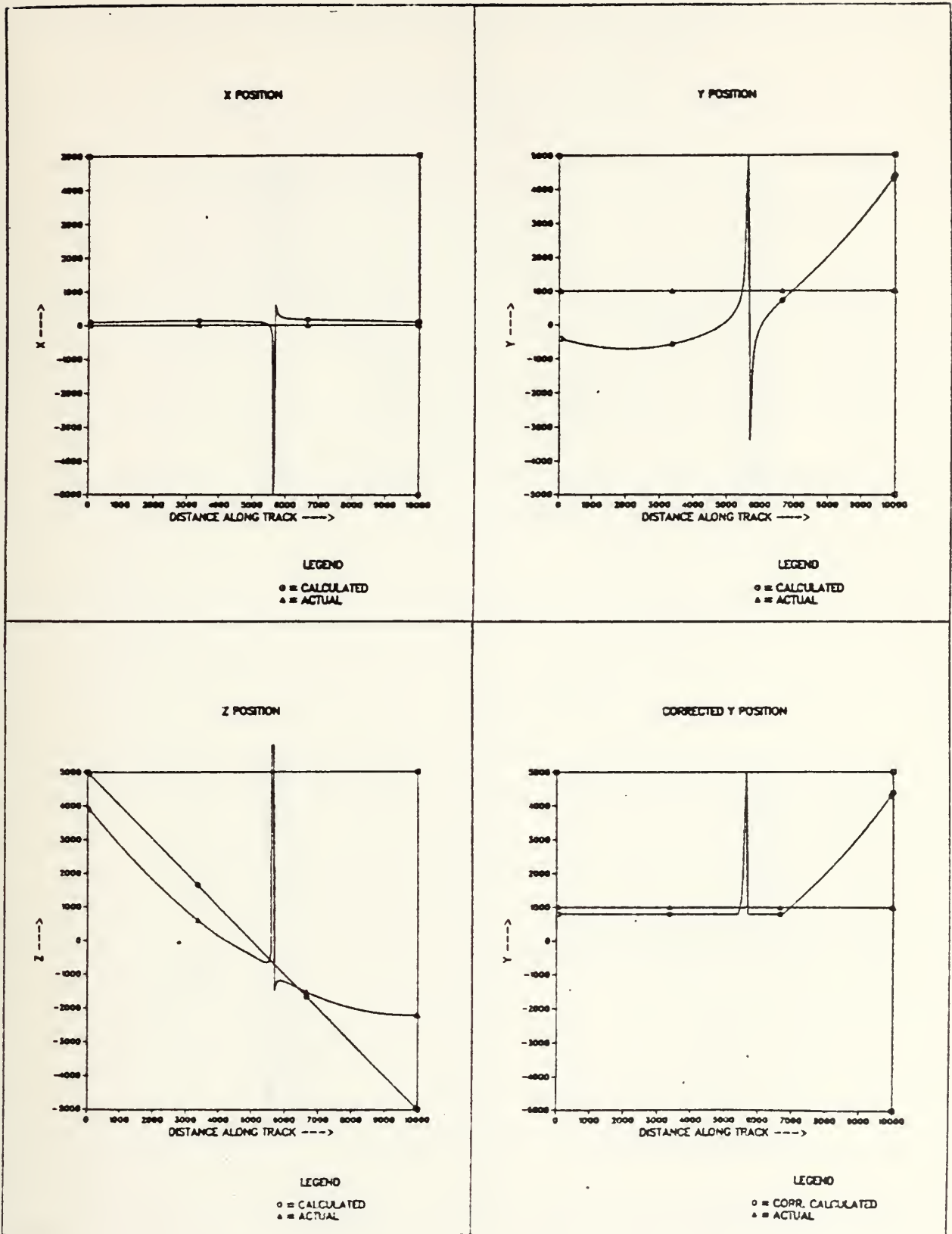


Figure 4.11 \vec{m} Vert. Comp. 50° Down, \vec{m} Hor. Comp. 30° Magnetic.

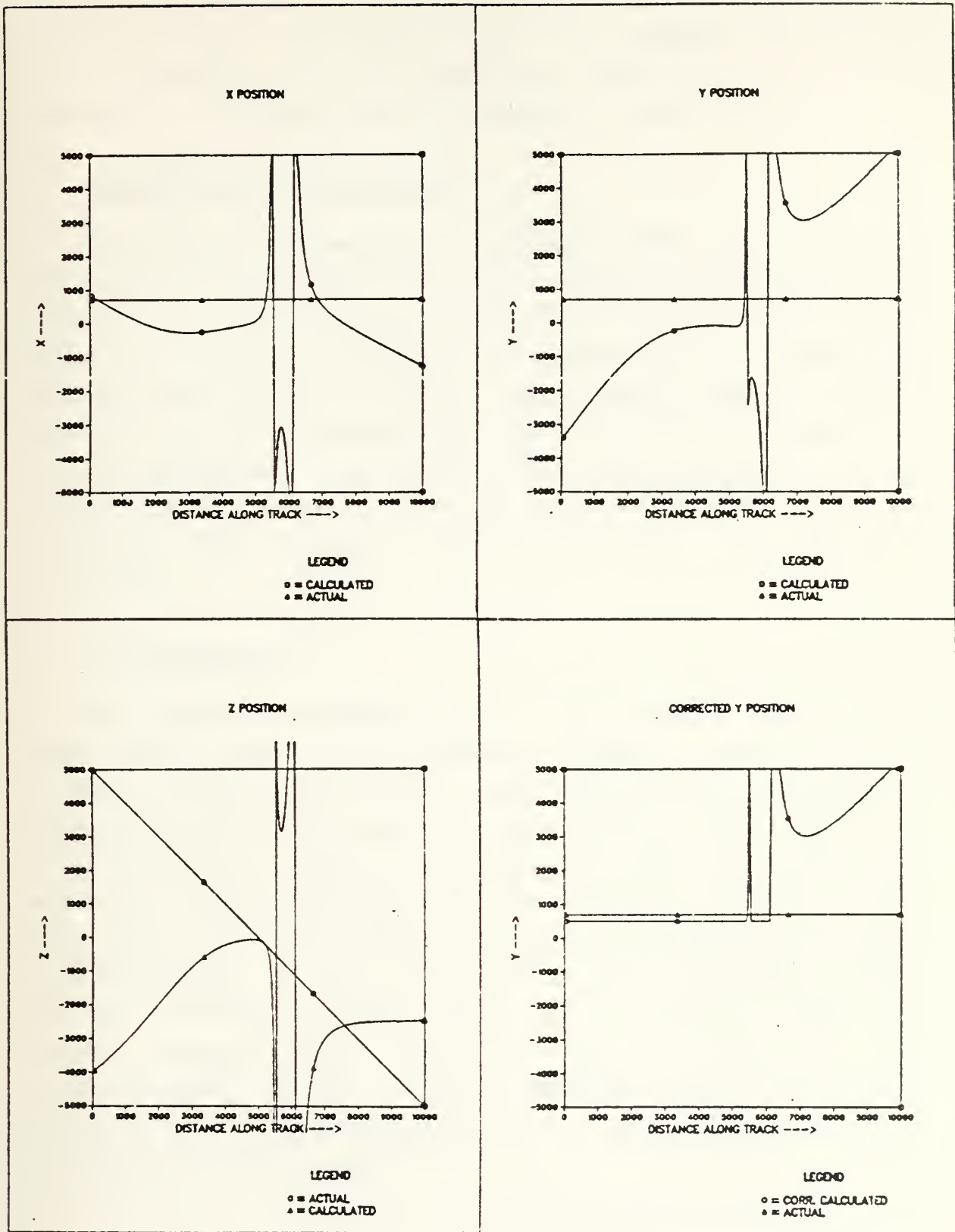


Figure 4.12 Target at 45° depres. angle rel. to platform at CPA.

cases, they do show reasonable values, and by themselves to provide limited localization data. The problem for inflight analysis would be to determine the bounds of a run in the absence of any other target positioning data.

H. IMPORTANCE OF CONSISTENCY

An important observation resulting from the analysis of the graphs, including those not shown as examples in this chapter, is that the rate of change of the calculated coordinates gives some indication of the validity of the positioning data. If the x and y graphs have a slope close to zero, and if the z graph has a slope of -45° for the calculated coordinate, then positioning data is likely to be comparatively accurate. If all three graphs fulfill this condition simultaneously, then positioning data appears to be usable.

I. IMPLEMENTATION

The possible implementation of the process described in this thesis would be to assume a magnetic moment for the target, then run the signal data through the processing to generate positioning data, and then compare these results to those obtained by using the assumed moment to generate a signal via this simulation. If the agreement between results were good, one could assume that one had assumed the correct target moment; if not, one would assume a different moment, and go through the process again, until one had a reasonable target moment, which would be valid at least until the target changed course. Using a computer these comparisons could be made reasonably quickly, so this process might have operational possibilities.

V. CONCLUSION

For the assumptions made, the positioning estimates are reasonable. Also, the averages taken of the three coordinates as calculated throughout the various runs show that the x calculation averages are in general at worst within 500 feet of the actual x value, while the worst y calculation averages tend to be within 1000 feet of the actual y value. The best calculated x and y values were within 100 and 200 feet, respectively, of the true values.

Trends observed were as follows:

1. It is best to fly the sensor platform directly over the target, or alternatively to have a 'distant' (between 1000 and 2000 foot) CPA off to one side while minimizing the target to platform separation in the y direction. The worst situation is when the target is at a point that, at CPA, has a depression angle of 45° with respect to the platform.
2. Best vertical separations are those that will yield a 500 to 1000 foot vertical distance between target and platform. Short vertical separations should be avoided if good localization is desired.
3. Best results are obtained if headings are northerly or southerly. Poor results are achieved with headings close to 60° , 120° , 240° , and 300° . East-West headings, while not as good as North-South, do provide good positioning data close to CPA.
4. Good results may be expected if there is a large vertical moment, especially if it is vertically up. Poor positioning results are obtained with this simulation if the moment has a large horizontal component.

5. Results are slightly better if the target moment is lined up with either the axis of flight or with the earth's field, although this effect is often dominated by the more gross effects caused by the other variables.

A suggested approach for further study is to inject noise into the simulation in order to see how robust it is in the accuracy of the position calculations. If the results remain reasonable, this approximation or an altered form of it may one day have real-world applicability.


```

M10000490
M10000500
M10000510
M10000520
M10000530
M10000540
M10000550
M10000560
M10000570
M10000580
M10000590
M10000600
M10000610
M10000620
M10000630
M10000640
M10000650
M10000660
M10000670
M10000680
M10000690
M10000700
M10000710
M10000720
M10000730
M10000740
M10000750
M10000760
M10000770
M10000780
M10000790
M10000800
M10000810
M10000820
M10000830
M10000840
M10000850
M10000860
M10000870
M10000880
M10000890
M10000900
M10000910
M10000920
M10000930
M10000940
M10000950
M10000960

```

```

MZ = 5.00*(DCOS(RALFA))*DCOS(RBETA))
EX = -(DCOS(RTHETA))*DSIN(RPHEE))
EY = DSIN(RTHETA)
EZ = (DCOS(RTHETA))*DCOS(RPHEE))
G = (MX*EX)+(MY*EY)+(MZ*EZ)
V1 = (3.00*MX*EX) - G
V2 = 3.00*((MX*EY)+(MY*EX))
V3 = (3.00*MY*EY) - G
V4 = (3.00*((MY*EZ)+(MZ*EY))
V5 = (3.00*MZ*EZ) - G
V6 = 3.00*((MX*EZ)+(MZ*EX))

```

```

C THE INITIAL POSITION OF SENSOR 1, AS WELL AS THE SENSOR SPACING
C DISTANCE "D" IS SET HERE -- IF A CHANGE IS DESIRED, THE PROGRAM
C MUST BE ALTERED AT THIS POINT.
C

```

```

X(1) = 0.00
Y(1) = 1000.00
Z(1) = -5000.00
D = 50.00
COB(1) = 0.0
COA(1) = 5000.0
COB(2) = 10000.0
COA(2) = 5000.0
COB(3) = 10000.0
COA(3) = -5000.0

```

```

C THE INITIAL POSITIONS OF SENSORS 2 - 5 ARE CALCULATED HERE.
C

```

```

X(2) = X(1) - D
Y(2) = Y(1) - D
X(3) = Y(1)
Y(3) = X(1)
X(4) = X(1) + D
Y(4) = Y(1)
X(5) = X(1)
Y(5) = Y(1)
Z(2) = Z(1)
Z(3) = Z(1)
Z(4) = Z(1) - D
Z(5) = Z(1)

```

30

```

C THE ACTUAL SIGNAL, BASED ON THE DIPOLE EQUATION, TO BE RECEIVED
C AT EACH OF THE FIVE SENSORS IS CALCULATED AT THIS POINT.
C

```

```

DO 20 J=1,5
RG = DSQRT((X(J)**2) + (Y(J)**2) + (Z(J)**2))
DOTIME = (MX*EX)+(MY*EY)+(MZ*EZ)

```



```

DOCTR = (MX*(J)) + (MY*(J)) + (MZ*(J))
DOURE = (X(J)*EX) + (Y(J)*EY) + (Z(J)*EZ)
TERM1 = (-DOTME)*(RG**2)
TERM2 = 3.0*DOTMR*DOURE
ANUM(J) = TERM1 + TERM2
TERM3 = 1.08 / (RG**5)
S(J) = TERM3 * (ANUM(J))
RNG(J) = RG
20 CONTINUE

```

```

C DIFFERENCES OF RECEIVED SIGNAL ARE TAKEN, IN ORDER TO ELIMINATE
C SQUARE AND HIGHER ORDER TERMS. THE DENOMINATOR IS ASSUMED TO BE
C THE SAME FOR THIS APPROXIMATION.

```

```

S2S3 = S(2) - S(3)
S2S5 = S(2) - S(5)
S3S1 = S(3) - S(1)
S3S4 = S(3) - S(4)
S5S4 = S(5) - S(4)

```

```

C THE RATIOS OF THE ABOVE DIFFERENCES ARE TAKEN IN ORDER TO
C ELIMINATE THE FIFTH-ORDER TERM IN THE DENOMINATOR.

```

```

A1 = S2S3/S2S5
A2 = S3S1/S5S1
A3 = S3S4/S5S4

```

EQUATION 3.1 COEFFICIENTS

```

C1 = (A1*(V2+(2.00*V1))) - (V2-(2.00*V1))
C2 = (A1*((2.00*V3)+V2)) - ((2.00*V3)-V2)
C3 = (A1*(V4+V6)) - (V4-V6)
K1 = ((V1-V3) - (A1*(V1-V3))) * D

```

EQUATION 3.2 COEFFICIENTS

```

C4 = (A2*2.00*V1) + (2.00*V1)
C5 = (A2*V2) + V2
C6 = (A2*V6) + V6
K2 = (V1 - (A2*V1)) * D

```

EQUATION 3.2 COEFFICIENTS

```

C7 = (A3*(V6+(2.00*V1))) - (V6-(2.00*V1))
C8 = (A3*(V4+V2)) - (V4-V2)
C9 = (A3*((2.00*V5)+V6)) - ((2.00*V5)-V6)
K3 = ((V1-V5) - (A3*(V1-V5))) * D

```

```

M1000970
M1000980
M1000990
M1001000
M1001010
M1001020
M1001030
M1001040
M1001050
M1001060
M1001070
M1001080
M1001090
M1001100
M1001110
M1001120
M1001130
M1001140
M1001150
M1001160
M1001170
M1001180
M1001190
M1001200
M1001210
M1001220
M1001230
M1001240
M1001250
M1001260
M1001270
M1001280
M1001290
M1001300
M1001310
M1001320
M1001330
M1001340
M1001350
M1001360
M1001370
M1001380
M1001390
M1001400
M1001410
M1001420
M1001430
M1001440

```



```

* ALONG TRACK ----> $, X ----> $) M1001930
CALL PLOTD (RZ, CX, 200, .FALSE., LINLIN, 'CALCULATED$', 'X POSITION$', M1001940
* DISTANCE ALONG TRACK ----> $) M1001950
CALL PLOTD (RZ, RX, 200, .TRUE., LINLIN, 'ACTUAL$', 'X POSITION$', 'DISTANCE', M1001960
* ANCE ALONG TRACK ----> $, X ----> $) M1001970
CALL PLOTD (COB, COA, 3, .FALSE., LINLIN, ' $', 'Y POSITION$', 'DISTANCE', M1001980
* ALONG TRACK ----> $, Y ----> $) M1001990
CALL PLOTD (RZ, CY, 200, .FALSE., LINLIN, 'CALCULATED$', 'Y POSITION$', M1002000
* DISTANCE ALONG TRACK ----> $, Y ----> $) M1002010
CALL PLOTD (RZ, RY, 200, .TRUE., LINLIN, 'ACTUAL$', 'Y POSITION$', 'DISTANCE', M1002020
* ANCE ALONG TRACK ----> $, Y ----> $) M1002030
CALL PLOTD (COB, COA, 3, .FALSE., LINLIN, ' $', 'Z POSITION$', 'DISTANCE', M1002040
* ALONG TRACK ----> $, Z ----> $) M1002050
CALL PLOTD (RZ, CZ, 200, .FALSE., LINLIN, 'CALCULATED$', 'Z POSITION$', M1002060
* DISTANCE ALONG TRACK ----> $, Z ----> $) M1002070
CALL PLOTD (RZ, RR, 200, .TRUE., LINLIN, 'ACTUAL$', 'Z POSITION$', 'DISTANCE', M1002080
* ANCE ALONG TRACK ----> $, Z ----> $) M1002090
CALL PLOTD (COB, COA, 3, .FALSE., LINLIN, ' $', 'CORRECTED Y POSITION$', M1002100
* DISTANCE ALONG TRACK ----> $, Y ----> $) M1002110
CALL PLOTD (RZ, YC, 200, .FALSE., LINLIN, 'CORR. CALCULATED$', 'CORR. Y', M1002120
* POSITION$, 'DISTANCE ALONG TRACK ----> $, Y ----> $) M1002130
CALL PLOTD (RZ, RY, 200, .TRUE., LINLIN, 'ACTUAL$', 'CORR. Y POSITION$', M1002140
* DISTANCE ALONG TRACK ----> $, Y ----> $) M1002150
CALL DONEPL M1002160
XAV = 0.0 M1002170
YAV = 0.0 M1002180
ZAV = 0.0 M1002190
DC 4 5 K = 1, 200 M1002200
XAV = XAV + CX(K) M1002210
YAV = YAV + CY(K) M1002220
ZAV = ZAV + CZ(K) M1002230
Z CONTINUE M1002240
AVGX = XAV/200 M1002250
AVGY = YAV/200 M1002260
AVGZ = ZAV/200 M1002270
WRITE (6, 60) M1002280
TX = -X(I) M1002290
TY = -Y(I) M1002300
WRITE (6, 85) TX, A VGX M1002310
FORMAT (IX, F7.1, ' IS THE TRUE X DISTANCE.', /IX, F7.1, ' IS THE AVERAG M1002320
* E CALCULATED X DISTANCE.') M1002330
WRITE (6, 86) TY, A VGY M1002340
FORMAT (IX, F7.1, ' IS THE TRUE Y DISTANCE.', /IX, F7.1, ' IS THE AVERAG M1002350
* E CALCULATED Y DISTANCE.') M1002360
WRITE (6, 73) AVGZ M1002370
FORMAT (IX, F7.1, ' IS THE AVERAGE CALCULATED Z VALUE.') M1002380
WRITE (6, 87) HEAD M1002390
FORMAT (IX, F7.1, ' IS THE PLATFORM HEADING.') M1002400

```

45

85

86

73

87


```

WRITE (6,88) EDIP
88 FORMAT (1X,F7.1, ' IS THE DIP ANGLE OF THE EARTH',1H', 'S MAGNETIC
* IELD, + IS DOWN. ')
DEG = 360.0 / C + HORM
IF (DEG.LT.360.0) GO TO 84
DEG = DEG - 360.0
84 WRITE (6,89) DIPM, DEG
89 FORMAT (1X,F7.1, ' IS THE DIP ANGLE OF THE TARGET',1H', 'S DIPCLE MOM
* MENT, + IS DOWN. /1X,F7.1, ' IS THE HORIZONTAL COMPONENT OF THE SAMM
* E. ')
WRITE (6,60)
60 FORMAT (1,1)
STOP
END

C
C
CRAMER'S RULE SUBROUTINE
SUBROUTINE SUBMAT (AX,AY,AZ,AA,BX,BY,BZ,BB,CX,CY,CZ,CC,XX,YY,ZZ)
REAL*8 AX,AZ,AA,BX,BY,BZ,BB,CX,CY,CZ,CC,XX,YY,ZZ,DD
7 FORMAT (1,1,26X, ' MATRIX CANNOT BE CALCULATED. ')
DD = AX*((BY*CZ) - (BZ*CY)) - BX*((AY*CZ) - (AZ*CY)) + CX*((AY*BZ) - (AZ
*BY))
IF (DD.NE.0.00) GO TO 98
WRITE (6,7)
GO TO 99
98 XX = (AA*((BY*CZ) - (BZ*CY)) - BB*((AY*CZ) - (AZ*CY)) + CC*((AY*BZ) - (
*Z*BY)))/DD
YY = (AX*((BB*CZ) - (BZ*CC)) - BX*((AA*CZ) - (AZ*CC)) + CX*((AA*BZ) - (
*Z*BB)))/DD
ZZ = (AX*((BY*CC) - (BB*CY)) - BX*((AY*CC) - (AA*CY)) + CX*((AY*BB) - (
*A*BY)))/DD
95 RETURN
END
MI002410
FM1002420
MI002430
MI002440
MI002450
MI002460
MI002470
MOM1002480
SAMM1002490
MI002500
MI002510
MI002520
MI002530
MI002540
MI002550
MI002560
MI002570
MI002580
MI002590
MI002600
AZM1002610
MI002620
MI002630
MI002640
MI002650
MI002660
MI002670
MI002680
MI002690
AM1002700
MI002710
MI002720
MI002730

```


APPENDIX B

COMPUTER PROGRAM FOR NUMERICAL OUTPUT

```

CCCCCCCCCCCCCCCCCCCCCCCCCCCCCCCCCCCCCCCCCCCCCCCCCCCCCCCCCCCC
C THIS PROGRAM DOES THE SAME JOB AS THE ONE IN APPENDIX A, BUT THE
C OUTPUT IS IN NUMERICAL FORM. IN ADDITION TO THE COMPARATIVE
C POSITIONS, THE ACTUAL COEFFICIENTS OF THE EQUATIONS GOING INTO
C THE CRAMER'S RULE SUBROUTINE ARE LISTED, AS ARE RATIOS OF THEM TO
C ESTABLISH THAT THEY ARE INDEED LINEARLY INDEPENDENT. THE RECEIVED
C SIGNAL STRENGTH AT EACH SENSOR IS ALSO COMPARED TO THE EXPECTED
C DENOMINATOR USING THE RANGE TO SENSOR 1 AS THE COMMON GIVEN
C AS THE SOLUTION HAVE THE APPROXIMATION. NOTE THAT THE POSITIONS
C AND THAT SAID POSITIONS ARE THE TARGET, NOT THE PLATFORM, AS THE
C ORIGIN, AND THAT SAID POSITIONS ARE THE PLATFORM'S POSITION.
CCCCCCCCCCCCCCCCCCCCCCCCCCCCCCCCCCCCCCCCCCCCCCCCCCCCCCCCCCCC
C REAL*8 MX,MY,MZ,EX,EY,EZ,X,Y,Z,D,S,RG,S2S3,S2S5,G,PI,RADN,RTHETA,
C *RPHEE,S3S1,S5S1,S3S4,A1,A2,A3,C1,C2,C3,C4,C5,C6,C7,C8,C9,K1,K2,K3,
C *S5S4,V1,V2,V3,V4,V5,V6,HALFA, RBETA
C REAL,KIK2,KIK3
C DIMENSION X(5),Y(5),Z(5),S(5),RNG(5),ANUM(5)
C
C THE SAME PARAMETERS AS FOR THE PROGRAM IN APPENDIX A ARE ENTERED
C HERE. THE ONLY DIFFERENCE IS THAT BETA, THE DIPOLE HORIZONTAL
C COMPONENT, IS INSERTED IN DEGREES COUNTER-CLOCKWISE FROM THE
C PLATFORM HEADING. ALL PARAMETER CHANGES IN THIS PROGRAM ARE NON-
C INTERACTIVE, AND MUST BE CHANGED IN THE PROGRAM ITSELF.
C
C PHEE = 30.
C THETA = 70.
C ALFA = 50.
C BETA = 35.
C PI = 4.00 * DATAN(1.00)
C RADN = PI / 180.00
C RTHETA = THETA * RADN
C RPHEE = PHEE * RADN
C KALFA = ALFA * RADN
C RBETA = BETA * RADN
C MX = (-5.00)*(DCOS(RALFA))*(DSIN(RBETA))
C MY = 5.00*(DSIN(RALFA))
C MZ = 5.00*(DCOS(RALFA))*(DCOS(RBETA))
C EX = -(DCOS(RTHETA))*(DSIN(RPHEE))
C EZ = (DCOS(RTHETA))*(DCOS(RPHEE))
C G = (MX*EX)+(MY*EY)+(MZ*EZ)
C V1 = (3.00 * MX*EX) - G
C V2 = (3.00 * MY*EY) + (MY*EX)
C V3 = (3.00 * MY*EY) - G
C V4 = (3.00 * MY*EZ) + (MZ*EY)
C V5 = (3.00 * MZ*EZ) - G
C
C MI100010
C MI100020
C MI100030
C MI100040
C MI100050
C MI100060
C MI100070
C MI100080
C MI100090
C MI100100
C MI100110
C MI100120
C MI100130
C MI100140
C MI100150
C MI100160
C MI100170
C MI100180
C MI100190
C MI100200
C MI100210
C MI100220
C MI100230
C MI100240
C MI100250
C MI100260
C MI100270
C MI100280
C MI100290
C MI100300
C MI100310
C MI100320
C MI100330
C MI100340
C MI100350
C MI100360
C MI100370
C MI100380
C MI100390
C MI100400
C MI100410
C MI100420
C MI100430
C MI100440
C MI100450
C MI100460
C MI100470
C MI100480

```



```

C
C
C
C
V6 = 3.D0 * ((MX*EZ) + (MZ*EX))
AS IN THE OTHER PROGRAM, SENSOR 1 INITIAL POSITION AND THE SENSOR
SPACING IS SET AT THIS POINT.

```

```

X(1) = 0.D0
Y(1) = -1000.D0
Z(1) = -5000.D0
D = 50.D0
X(2) = X(1)
Y(2) = Y(1) - D
X(3) = X(1)
Y(3) = Y(1) - D
X(4) = X(1)
Y(4) = Y(1)
X(5) = X(1) + D
Y(5) = Y(1)
Z(2) = Z(1)
Z(3) = Z(1)
Z(4) = Z(1) - D
Z(5) = Z(1)
DO 20 J=1,5
RG = DSQR((X(J)**2) + (Y(J)**2) + (Z(J)**2))
DOIME = (MX*EX) + (MY*EY) + (MZ*EZ)
DOIMR = (MX*X(J)) + (MY*Y(J)) + (MZ*Z(J))
DOIRE = (X(J)*EX) + (Y(J)*EY) + (Z(J)*EZ)
TERM1 = (-DOIME)**(RG**2)
TERM2 = 3.*DOIMR*DOIRE
ANUM(J) = TERM1 + TERM2
TERM3 = 1.C8 / (RG**5)
S(J) = TERM3 * (ANUM(J))
RNG(J) = RG
CGN(J) = RG

```

```

20
AVRNG = RNG(1)
DNOM = 1.D8 / (AVRNG**5)
S1 = ANUM(1) * DNOM
S2 = ANUM(2) * DNOM
S3 = ANUM(3) * DNOM
S4 = ANUM(4) * DNOM
S5 = ANUM(5) * DNOM
APP25 = S2 - S3
APP31 = S3 - S1
APP51 = S5 - S1
APP34 = S3 - S4
APP54 = S5 - S4
FORMAT ('X', 'ACTUAL', '8X', 3F10.2)
FORMAT ('EQNS', '25X', 'X', '9X', 'Y', '9X', 'Z')

```

```

M1100490
M1100500
M1100510
M1100520
M1100530
M1100540
M1100550
M1100560
M1100570
M1100580
M1100590
M1100600
M1100610
M1100620
M1100630
M1100640
M1100650
M1100660
M1100670
M1100680
M1100690
M1100700
M1100710
M1100720
M1100730
M1100740
M1100750
M1100760
M1100770
M1100780
M1100790
M1100800
M1100810
M1100820
M1100830
M1100840
M1100850
M1100860
M1100870
M1100880
M1100890
M1100900
M1100910
M1100920
M1100930
M1100940
M1100950
M1100960

```



```

71 FORMAT (' USED',24X,'POS',7X,'POS',7X,'POS')
60 FORMAT (' ',S(2),S(3),S(4),S(5))
S2S3 = S(2) - S(3)
S2S5 = S(2) - S(5)
S3S1 = S(3) - S(1)
S5S1 = S(5) - S(1)
S3S4 = S(3) - S(4)
S5S4 = S(5) - S(4)
A1 = S2S3/S2S5
A3 = S3S1/S5S1
A3S4 = S3S4/S5S4
C1 = (A1*(V2+(2.D0*V1)) - (V2-(2.D0*V1)))
C2 = (A1*((2.D0*V3)+V2)) - ((2.D0*V3)-V2)
C3 = (A1*((V4+V6)) - (V4-V6))
K1 = ((V1-V3) - (A1*(V1-V3))) * D
C4 = (A2*2.D0*V1) + (2.D0*V1)
C5 = (A2*V2) + V2
C6 = (A2*V6) + V6
K2 = (V1 - (A2*V1)) * D
C7 = (A3*(V6+(2.D0*V1))) - (V6-(2.D0*V1))
C8 = (A3*((V4+V2)) - (V4-V2))
C9 = (A3*((2.D0*V5)+V6)) - ((2.D0*V5)-V6)
K3 = ((V1-V5) - (A3*(V1-V5))) * D

```

C THE BELOW LISTED VARIABLES ARE THE RATIOS OF THE COEFFICIENTS
C USED TO SHOW LINEAR INDEPENDENCE OF THE THREE EQUATIONS.
C

```

K1K2 = K1/K2
K1K3 = K1/K3
K2K3 = K2/K3
C1C4 = C1/C4
C2C5 = C2/C5
C3C6 = C3/C6
C1C7 = C1/C7
C2C8 = C2/C8
C3C9 = C3/C9
C4C7 = C4/C7
C5C8 = C5/C8
C6C9 = C6/C9
WRITE (6,60)
WRITE (6,60)
WRITE (6,60)
WRITE (6,60)
WRITE (6,110)
110 *IX,EQUATION,4X,CONSTANT,8X,SENSED,8X,CALCULATED,10X,'|',1
WRITE (6,111)
111 FORMAT (' NUMBER',7X,'RANGE',8X,'SIGNAL',10X,'|',12X,'|',12X,

```



```

REAL*8 AX,AY,AZ,AA,BX,BY,BZ,BB,CX,CY,CZ,CC,XX,YY,ZZ,DD
7  FORMAT ('+',26X,'MATRIX CANNOT BE CALCULATED.!',
  *BY))
  DD = AX*((BY*CZ) - (BZ*CY)) - BX*((AY*CZ) - (AZ*CY)) + CX*((AY*BZ) - (AZ
  *BY))
  IF (DD.NE.C.00) GO TO 98
  WRITE (6,7)
  GO TO 99
98  XX = (AA*((BY*CZ) - (BZ*CY)) - BB*((AY*CZ) - (AZ*CY)) + CC*((AY*BZ) - (A
  *Z*BY)))/DD
  YY = (AX*((BB*CZ) - (BZ*CC)) - BX*((AA*CZ) - (AZ*CC)) + CX*((AA*BZ) - (A
  *Z*BB)))/DD
  ZZ = (AX*((BY*CC) - (BB*CY)) - BX*((AY*CC) - (AA*CY)) + CX*((AY*BB) - (A
  *A*BY)))/DD
  WRITE (6,2) XX,YY,ZZ
2  FORMAT ('10X,'CALCULATED',4X,3F10.2)
  WRITE (6,60)
60  FORMAT ('+',
  *')
99  RETURN
  END
M1101930
M1101940
M1101950
M1101960
M1101970
M1101980
M1101990
M1102000
M1102010
M1102020
M1102030
M1102040
M1102050
M1102060
M1102070
M1102080
M1102090
M1102100
M1102110

```


APPENDIX C

EXAMPLE OUTPUT OF APPENDIX B

An example of the output of the program in Appendix B is shown below. The total output for a single time step is presented.

SENSOR NUMBER	SLANT RANGE	SENSED SIGNAL	CALCULATED SIGNAL
1	5050.0	0.6054D-04	0.6054E-04
2	5060.1	0.1556D-03	0.1612E-03
3	5050.2	0.2682D-04	0.2683E-04
4	5099.0	0.3940D-04	0.4135E-04
5	5050.2	0.9366D-04	0.9368E-04

ECLATION	TRUE	APPROXIMATE
S2-S3	0.1327E-03	0.1343E-03
S2-S5	0.6590E-04	0.6748E-04
S3-S1	-0.3372E-04	-0.3371E-04
S5-S1	0.3312E-04	0.3314E-04
S3-S4	-0.1258E-04	-0.1452E-04
S5-S4	0.5426E-04	0.5233E-04

EQNS USED	X POS	Y POS	Z POS
1 2 3	0.0	-1000.00	-4950.00
-----	ACTUAL		
-----	CALCULATED	-60.98	-870.83
-----			-4739.97

The first five rows of data above are for the appropriate "sensor" as indicated, the slant range from that sensor to the target, the received signal as generated by equation 2.5 and the signal that would be generated using the approximation described in Chapter 3 to linearize the problem. The next six rows show the results of taking the differences between the received and calculated (for comparison purposes only) signals, listed under the headings of TRUE and APPROXIMATE, respectively. The final two lines show the actual coordinates of the platform relative to the target (the coordinate transformation has not been done at this point) as compared to the calculated position. These are the points used by the program in Appendix A to plot the graphs after the coordinate transformation is completed.

The second section of the output is shown below.

EQUATION NUMBER	CONSTANT	X COEFFICIENT	Y COEFFICIENT	Z COEFFICIENT
1	0.50D+03	-0.30D+02	-0.92D+01	0.20D+01
2	-0.38D+03	0.14D+00	0.13D+00	0.54D+01
3	-0.85D+02	-0.21D+01	-0.19D+02	0.35D+01
RATIO				
1/2	-0.13E+01	-0.22E+03	-0.71E+02	0.36E+02
1/3	-0.58E+01	0.14E+02	0.49E+00	0.56E+00
2/3	0.44E+01	-0.65E-01	-0.69E-02	0.15E-01

The first three lines of the output represent the coefficients of the equations 3.6 - 3.8 in the form of $CONSTANT = X \text{ COEFF}(x) + Y \text{ COEFF}(y) + Z \text{ COEFF}(z)$. In order to determine the linear independence of these equations, the ratios of the coefficients are taken in pairs. Since it may be seen from the last three lines of the output that the ratios of the constants and coefficients differ significantly for all three equations, it can be concluded that the equations are linearly independent. This holds true throughout any given run, which may be verified by printing out all time steps for that run.

APPENDIX D
CRAMER'S RULE

A. GENERAL

Cramer's Rule, a method for solving systems of linear equations in two or more unknowns, states that each unknown can be expressed as the ratio of two determinates. The general form of a solution is shown below.

$$Ax+By+Cz=0$$

$$Ex+Fy+Gz=H$$

$$Ix+Jy+Kz=L$$

$$D = \begin{vmatrix} A & B & C \\ E & F & G \\ I & J & K \end{vmatrix}$$

$$x = \begin{vmatrix} 0 & B & C \\ H & F & G \\ L & J & K \end{vmatrix} / D$$

$$y = \begin{vmatrix} A & 0 & C \\ E & H & G \\ I & L & K \end{vmatrix} / D$$

$$z = \begin{vmatrix} A & B & 0 \\ E & F & H \\ I & J & L \end{vmatrix} / D$$

B. EXAMPLE

The following example was taken from [Ref. 4]. Solve:

$$3x-2y+2z=7$$

$$x+ y+ z=6$$

$$2x- y-2z=2$$

Let D be the denominator.

$$D = \begin{vmatrix} 3 & -2 & 2 \\ 1 & 1 & 1 \\ 2 & -1 & -2 \end{vmatrix} = -17$$

$$x = \frac{\begin{vmatrix} 7 & -2 & 2 \\ 6 & 1 & 1 \\ 2 & -1 & -2 \end{vmatrix}}{D} = \frac{-51}{-17} = 3$$

$$y = \frac{\begin{vmatrix} 3 & 7 & 2 \\ 1 & 6 & 1 \\ 2 & 2 & -2 \end{vmatrix}}{D} = \frac{-34}{-17} = 2$$

$$z = \frac{\begin{vmatrix} 3 & -2 & 7 \\ 1 & 1 & 6 \\ 2 & -1 & 2 \end{vmatrix}}{D} = \frac{-17}{-17} = 1$$

CHECK:

$$3x - 2y + 2z = 7$$

$$3(3) - 2(2) + 2(1) = 7$$

$$9 - 4 + 2 = 7$$

$$7 = 7$$

$$x + y + z = 6$$

$$3 + 2 + 1 = 6$$

$$6 = 6$$

$$2x - y - 2z = 2$$

$$2(3) - 2 - 2(1) = 2$$

$$6 - 2 - 2 = 2$$

$$2 = 2$$

C. SUBROUTINE "CRAMER'S RULE" CHECK

Running the values in Section B through the subroutines of the programs in Appendix A and Appendix B yielded the same results as the example.

LIST OF REFERENCES

1. Wynn, W.M., Frahm, C.P., Carroll, P.J., Clark, R.H.,
Wellhoner, J., Wynn, M.J., Advanced Superconductive
gradiometer/magnetometer arrays and a novel signal
processing technique p.707-707, IEEE Trans.
Magnetics, MAG-11, 1975
2. Fromm, W.E., in Advances in Electronics, V.4, edited by
Marton, L., p.260, Academic Press, 1952
3. Reitz, J.R., Milford, F.J., p.164, Foundations of
Electromagnetic Theory, Addison-Wesley
Publishing Co., Inc., 1967
4. Shapiro, M.S., Mathematics Encyclopedia, p.49,
Doubleday & Company, Inc., 1977
5. Anderson, J.E., NADC Report NADC-EL-47-50, Magnetic
Airborne Detection Frequency Responses, 1949

BIBLIOGRAPHY

- BOEING Aerospace Company Proprietary Data, NAVY/BOEING Development of a Dual MAD Localization System, 8 November 1974
- BOEING Aerospace Company, Dual MAD Processing Study, Task 1 Report, Advanced MEG Program, 1 November 1976
- BOEING Aerospace Company, Dual MAD Processing Study, Task 2 Report, Techniques Analysis, 1 December 1976
- National Defense Research Committee Division 6 Technical Report, Magnetic Airborne Detection Program, V.5, 1946
- Naval Air Development Center Technical Memorandum NADC-3012:ARO, Extrema, symmetry, and zeroes of MAD signals and their application to MAD localization, 20 October 1982
- TEXAS INSTRUMENTS INCORPORATED, Analysis of Transverse Gradiometer MAD using Dual Scalar Magnetometers, Part I: Detection Model and Performance, McGregor, D., July 1976
- TEXAS INSTRUMENTS INCORPORATED, Analysis of Transverse Gradiometer MAD using Dual Scalar Magnetometers, Part II: Tactical Parameter Extraction, McGregor, D., January 1978
- TEXAS INSTRUMENTS INCORPORATED, Flight Test Plan Dual MAD, McGregor, D., undated

INITIAL DISTRIBUTION LIST

		No. Copies
1.	Fleet Tactical Library P.O.Box 1042 Silver Springs, Md. 20910	2
2.	Defense Technical Information Center Cameron Station Alexandria, Virginia 22314	2
3.	Library, Code 0142 Naval Postgraduate School Monterey, Ca. 93943	2
4.	Dr. R. N. Forrest, Code 71 Chairman ASW Academic Group Naval Postgraduate School Monterey, Ca. 93943	2
5.	Dr. Otto Heinz, Code 61Hz Department of Physics Naval Postgraduate School Monterey, Ca. 93943	2
6.	Dr. Andrew R. Ochadlick, Jr., Code 610c Department of Physics Naval Postgraduate School Monterey, Ca. 93943	2
7.	LCDR C. Burmaster, USN, Code 612r Department of Physics Naval Postgraduate School Monterey, Ca. 93943	1
8.	LT Wolf H. Bock, USN ASWOC Sigonella FPO New York, N.Y. 09523	2
9.	Mr. John Shannon Naval Air Development Center (Code 3012) Warminster, Pa. 18974	1
10.	Mr. Edward Yannuzzi Naval Air Development Center (Code 30) Warminster, Pa. 18974	1
11.	Chief of Naval Research Department of the Navy Attn: John G. Heacock (Code 425 GG) 800 North Quincy Street Arlington, Va. 22217	1
12.	Mr. William Andahazy Naval Ship Research & Development Center Annapolis Laboratory Annapolis, Md. 21402	1

Thesis

202580

Thesis

B58895

Bock

c.1

A linear approximation of the source position using multiple MAD.

7 SEP 90

37053

Thesis

202580

B58895

Bock

c.1

A linear approximation of the source position using multiple MAD.



3 2768 00018676 1